The Thesis Committee for Carlos Galdeano Alexandres
Certifies that this is the approved version of the following thesis:

Modeling Stormwater Sewer Systems using High Resolution Data

APPROVED BY
SUPERVISING COMMITTEE:

Supervisor:

David R. Maidment

Daene C. McKinney

Modeling Stormwater Sewer Systems using High Resolution Data

by

Carlos Galdeano Alexandres

Thesis

Presented to the Faculty of the Graduate School of

The University of Texas at Austin

in Partial Fulfillment

of the Requirements

for the Degree of

Master of Science in Engineering

The University of Texas at Austin

May 2014

Dedication

I would like to dedicate this thesis to my family and friends. In particular, to my wife who encouraged me to follow my dreams. Thank you!

Acknowledgements

I would like to thank the government of Mexico who supported this project through the National Council of Science and Technology (CONACyT). I am deeply grateful to my advisor Dr. Maidment for his guidance, energy and experience throughout this work. Moreover, I would like to thank Denny Rivas, Gonzalo Espinoza, Amanda Cuellar, and Georges Comair for their assistance and valuable point of view during my master's studies.

I would also like to express my deep gratitude to my undergraduate professors at the UNAM, who gave me the tools and mentality needed to succeed in my graduate studies. Finally, I would like to thank all my coworkers at the Center for Research in Water Resources (CRWR), and the EWRE faculty and students.

Abstract

Modeling Stormwater Sewer Systems using High Resolution Data

Carlos Galdeano Alexandres, M.S.E

The University of Texas at Austin, 2014

Supervisor: David R. Maidment

More than 54% of the world population lives in urban areas, and this percentage is projected to increase rapidly in future years. This growth significantly affects the hydrological cycle, which translates into social and economic costs due to urban flooding. This thesis develops a procedure to evaluate the current storm water infrastructure using Airborne LiDAR data. This evaluation is essential to mitigate and prevent the effect of floods in urban areas. Airborne LiDAR data provides the elevation data necessary to characterize the elements involved in the storm water system. The processing of this data, digitization, and characterization of the storm drainage system is computed with ArcGIS, Geographic Information System (GIS) software. Scenarios for 4 return periods (2, 10, 25 and 100 years) are modeled using StormCAD in order to evaluate the capacity of the stormwater sewer system in the northwest area of The University of Texas at Austin main campus. The performance of the drainage system might work under strain for a 100-year storm event; therefore, it is suggested to modify the pipe sizes to prevent flooding in the area analyzed. The results indicate that the methodology proposed for evaluating the current conditions of a stormwater drainage system produces valid results, but can be improved using Ground-based LiDAR data.

Table of Contents

List of Tables

List of Figures

Chapter 1: Introduction

1.1 Overview

Water is a chemical compound that covers almost 71% of the Earth, vital for living things, and a major force that shapes the surface of the Earth (Chow et al., 1988). Hydrology is the science that describes the circulation and distribution of the water on the Earth and its atmosphere. This science has two principal focuses: 1) The global hydrologic cycle, and 2) The land phase of the hydrologic cycle. The first studies the distribution and variations (temporal and spatial) of water in terrestrial, oceanic, and atmospheric areas of the water system. The second describes the movement of water in the Earth's surface and groundwater, the interactions with Earth's materials, and the biological processes that conduct or affect that movement (Dingman 2014).

The hydrologic cycle in urban areas behaves in a similar way as for the global perspective, but the proportion of infiltrated water varies depending on the percentage of impervious surfaces. An increase in impervious surface will induce an increase in surface runoff, a decrease in evaporation, and a decrease in infiltration. The increase in surface runoff in urban areas has to be managed in order to prevent urban floods caused by stormwater. Urban floods are a global problem that causes extensive devastation, economic damage and loss of human lives. According to the National Oceanic and Atmospheric Administration (NOAA), losses caused by floods average $8.17 Billion USD in economic damage and 89 deaths per year in the United States over the last 30 years.

Three common approaches to prevent urban flooding from stormwater are 1) The stormwater conveyance approach, 2) The stormwater infiltration approach, and 3) The storage approach. The stormwater conveyance approach involves the fast removal of

stormwater from impervious surfaces to receiving streams by means of stormwater sewer systems. The stormwater infiltration approach involves the capture of stormwater, and the infiltration to the extent possible into the soil through greenroofs, rainbarrels, streetside raingardens, porous paving, etc. (Novotny et al., 2010). The storage approach involves the capture and storage of stormwater using detention ponds.

The purpose of stormwater sewer systems is to remove water from the site as quickly and efficiently as possible. In some cases, because of poorly planned systems or quick urban growth, urban floods are caused by inefficient stormwater sewer systems. Current methodologies for modeling these systems rely on 2-D data such as blueprints and contours. These methodologies do not include high-resolution spatial data to assess and visualize global geospatial conditions. These methodologies can be adapted by combining Geographic Information Systems (GIS) and integrating Light Detection and Ranging (LiDAR) data in order to build dynamic and precise models. GIS offers the tools to process, digitize, characterize and analyze geospatial data. On the other hand, LiDAR data provides high-resolution elevation data that helps describe the landscape, which in turn provides a better understanding of the interaction between stormwater and urban areas.

In several lectures, Dr. David Maidment (Hussein M. Alharthy Centennial Chair in Civil Engineering at The University of Texas at Austin) has introduced an innovative approach he developed called "HydroDesign", which is a subset of GeoDesign. GeoDesign is define by Steinitz (2012) as "the development and application of design related procedures intended to change the geographical study areas in which they are applied and realized", while HydroDesign is as a method of evaluating and planning the way people interact with water in their surroundings. HydroDesign is related to another concept called The Digital Campus of The University of Texas at Austin (UT), which

moves towards 3-D representation of the main campus of UT using specialized software such as ESRI's City Engine. The Digital Campus is a compilation of data that describes the three-dimensional layout and environmental conditions of the campus, which will incorporate the HydroDesign concept. One important goal of HydroDesign is to mitigate the impacts of flooding. Consequently, it is imperative to build dynamic and precise stormwater sewer system models to evaluate the existing conditions and develop future sustainable plans.

1.2 OBJECTIVES

The purpose of the present work intends to understand and evaluate the following research questions:

a. Can HydroDesign be developed from GeoDesign?

b. Can a 3-D model of UT's main campus be constructed? If so, how could it be used to support this process?

c. How does Ground-based LIDAR data improve the terrain representation compared to Airborne LIDAR data?

In order to answer these research questions, this thesis develops a procedure for modeling and analyzing current urban stormwater systems using GIS and Airborne LiDAR data. This procedure will help model a specific stormwater sewer system that can be incorporated into The Digital Campus. Furthermore, this thesis presents a case study of a stormwater sewer system for the northwestern area of UT's main campus, which can be integrated into the larger Digital Campus.

Chapter 2: Literature and Technology Review

2.1 Geographic Information Systems

Geographic information systems (GIS) represent in maps data referenced to geographic co-ordinates (Curran, 1984). GIS assist in the capture, storage, manipulation, and analysis of the information pertinent to geospatial features which are linked to tables that contain their attributes. Environmental Systems Research Institute (ESRI) is one of the most important developers of GIS software. ESRI's suite of GIS geospatial processing software is referred to as ArcGIS, which can operate in desktop and online environments. The desktop products are ArcMap, ArcCatalog, ArcScene, ArcGlobe, Arc Toolbox, and ArcReader. The features in these products are also known as feature classes or shapefiles. Feature classes are features stored in geodatabases, while the shapefiles are stored in folders. A geodatabase is a storage framework that combines the spatial data and the data repository. In general, ArcGIS products are used for viewing, editing, creating, and analyzing geospatial features, allowing us to represent these features in maps. In particular, ArcMap allows us to represent geospatial features in maps in a plan view, while ArcScene does so in 3-D.

2.1.1 GIS in Water Resources

Hydrologists use large amounts of data to determine water supply, mitigate floods, evaluate water quality, and manage water resources. These data are hard to store, visualize, and process (Maidment 2002). GIS software offers tools that speed up and simplify the management of hydrologic data, changing the way hydrologists handle water resources management and modeling. In 2002, the Center for Research in Water Resources (CRWR) and ESRI developed a geospatial and temporal data model for water resources known as ArcHydro. ArcHydro is a module within ArcGIS that offers a shared

structure to link hydrologic features (Maidment, 2002). The most common applications of GIS in water resources are 1) Surface Water Hydrologic Modeling, 2) Water Supply and Sewer Systems Modeling, and 3) Groundwater Modeling. Surface Water Hydrologic Modeling represents the effects of rainfall and runoff on the surface of the earth, which requires information describing the land use, topography, and type of soil obtained by GIS. Water Supply and Sewer Systems Modeling rely on GIS to display maps that contain the information to plan, design, analyze, operate and maintain water and sewer systems in metropolitan areas in a sustainable and optimal way. Groundwater Modeling represents the storage, movement, and water quality of groundwater in an aquifer, and requires information that describes the soil water storage, type of soil, topography, and aquifer characteristics (Tsihrintzis et al., 1995).

2.1.2 GeoDesign and HydroDesign

In 2009, Jack Dangermond, the President of ESRI, wrote an article on ArcNews online (ESRI blog) titled "GIS: Designing Our Future". In this article, he introduced the concept of "GeoDesign", which brings geographic analysis into the design process that allowing assessing and visualizing almost immediately the effects of different design alternatives. In other words, GeoDesign enables the resources of natural systems to be optimized to benefit humans and nature through a more sustainable coexistence. According to Dangermond, GeoDesign comprises the activity spaces of 1) the work environment, 2) the design tools, and 3) supportive workflows. The first refers to the locations where geo-based design professionals do their work that includes desktops, servers, databases, collaborative environments, etc. The second refers to the tools used by these designers to create their designs, and the third to the manner in which these designers do their work.

Steinitz (2012) developed the GeoDesign framework that enlists the steps, methods, and strategies for regional land-use design projects. This framework looks to incorporate all the requirements of the participants involved in the project, especially the posed by the people of the place, institutions, and stakeholders. In case any of the requirements of the participants are not satisfied, alternatives have to be developed. The framework for GeoDesign involves a series of six questions that are answered with different models. These questions are asked and answered at least three times during the design process of the project. As Figure 2.1 shows, the questions and models to answer them are the following:

1) How should the study area be described? This question has to be answered using a representation model.
2) How does the study area operate? A process model has to be used to answer this question.
3) Is the current study area working well? An evaluation model has to be used to address this question.
4) How might the study area be altered? This question has to be addressed with a change model.
5) What differences might the changes cause? An impact model is used to answer this question.
6) How should the study area be changed? This question is addressed using a decision model.

The three iterations of questions and answers through this framework proposed by Steinitz (2012) follow the sequence shown in Figure 2.1. In the first iteration these questions are treated as "Why" questions starting from the 1st to the 6th question, which assists to understand the geographic location and scope of the project. In the second

iteration the six questions are treated as "How" questions and asked in reverse order, which assist to define the methods needed in the project. The second iteration helps the process to be decision-driven instead of data-driven. In the third iteration the six questions are asked to address the "What", "Where", and "When" questions and are examined from the 1st to the 6th question. During the third iteration the data needed for the project is identified, gathered, organized, and represented in the format needed for the project purposes, which allows implementing the project and providing results.

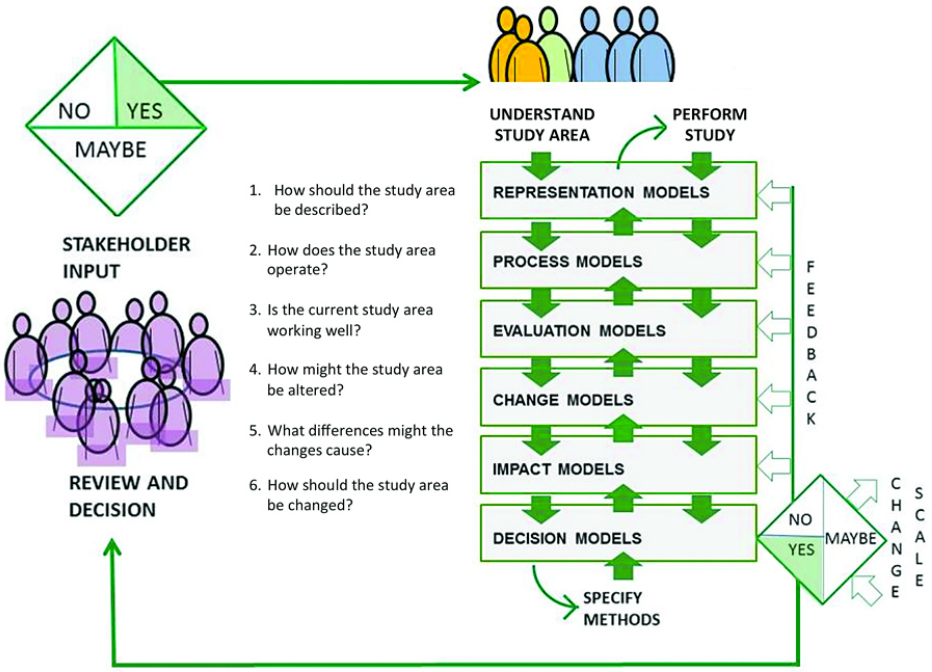

Figure 2.1: The framework for GeoDesign, including stakeholders and design team (Steinitz 2012).

During several lectures, Dr. David Maidment (Hussein M. Alharthy Centennial Chair in Civil Engineering at the University of Texas at Austin) introduced and defined a parallel concept to GeoDesign called "HydroDesign". HydroDesign refers to the application of the framework of GeoDesign to assess and design the way people

interrelate with water in constructed and natural environments. Furthermore, HydroDesign improves the design process, benefiting both humans and the environment. In other words, HydroDesign helps to 1) mitigate floods, 2) use water efficiently, and 3) prevent water pollution. The framework for HydroDesign can follow the outline of GeoDesign, which is based on the three iterations of six questions and answers presented in Figure 2.1. This framework has to be shaped for the requirements and needs of users, stakeholders, and institutions involved in the decision and design process of water management projects.

In particular, the framework for HydroDesign can be focused to mitigate floods by assessing, designing, and implementing appropriate urban stormwater sewer systems. The purpose of these systems is to remove water from the site rapidly and efficiently as possible to prevent floods. The main tools to design these systems are GIS and hydraulic-modeling software. On one hand, GIS software helps generate physical geospatial models for estimating the runoff response in urbanized catchments (Meyer et al., 1993). Furthermore, the use of GIS for urban stormwater systems modeling includes the creation, modification, and description of the geospatial features involved in stormwater sewer systems. On the other hand, hydraulic-modeling software, such as StormCAD, provides the simulation of the stormwater sewer system's elements response to different storm scenarios. The results obtained from the stormwater modeling software assist in generating the models needed to answer the questions during the three iterations of the HydroDesign framework.

2.2 DIGITAL TERRAIN MODEL

The Digital Terrain Model (DTM) is the digital numerical representation of the ground surface by points or cells with X, Y, and Z coordinates in an arbitrary coordinate system. Figure 2.2 shows a 3-D graphic representation of a DTM. In general, a DTM contains specific features such as 1) variety of forms of representation (e.g. topographic maps, cross sections, and 3-D views), 2) accuracy of data over time, 3) ability to update and integrate data at any time, and 3) easy multi-scale representation of different resolutions and scales (Li et al., 2005). Two alternatives to represent DTMs are as raster files or Triangulated Irregular Networks (TINs).

Common methods to collect the data needed to build the DTMs are 1) field measurement, usually done with a Global Position System (GPS) in addition to a total station theodolite for physical measurement of terrain surfaces; 2) photogrammetry, which uses stereo pairs of aerial or space images and photogrammetric instruments; 3) cartographic digitization, which employs physical topographic maps and digitizers; and recently 4) laser scan, which is a new and popular method that uses lasers as remote sensing instruments.

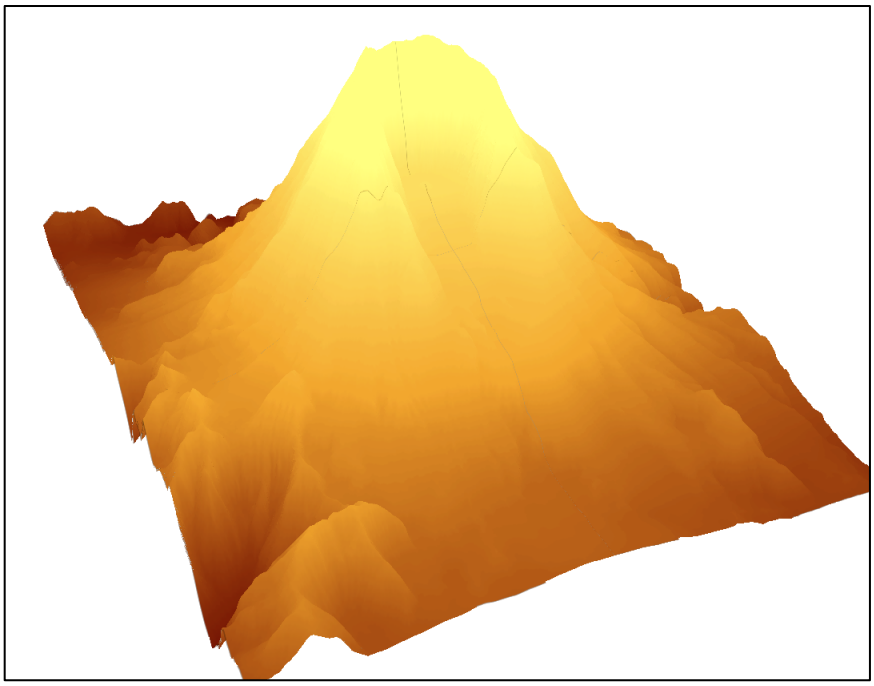

Figure 2.2: DTM 3-D Graphic representation of Mount St. Helens after 5/18/80 eruption (USGS 2006).

2.2.1 Digital Elevation Model Raster

Since the development of DTMs, other alternatives have been brought into use. One alternative is the Digital Elevation Model (DEM) that is widely used in America (Li et al., 2005). A Digital Elevation Model (DEM) is generally represented in the form of a raster. As shown in Figure 2.3, a DEM raster is a cellular-based elevation data arrangement formed by square cells of equal size arranged in rows and columns. Each cell of a DEM raster contains an elevation value that represents the height above a given level. A single cell of a DEM raster is analogous to a data point, while a zone of cells is equivalent to a polygon.

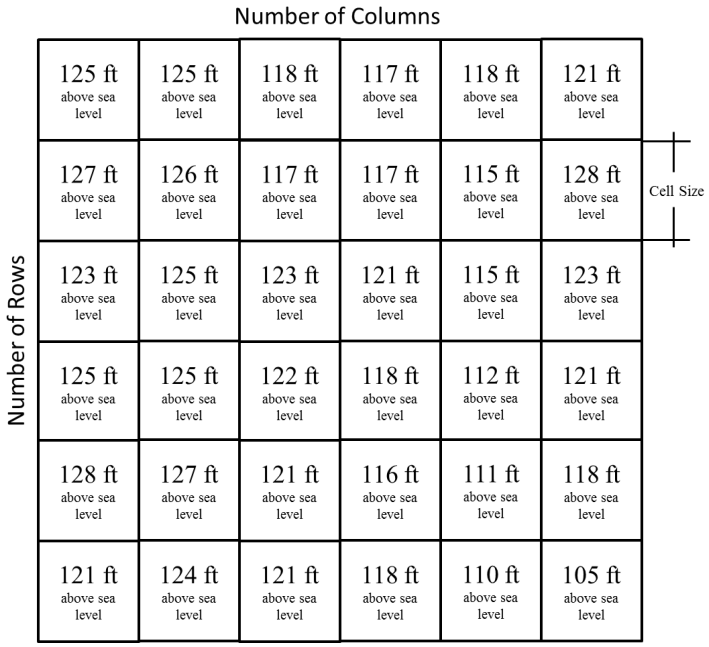

Figure 2.3: DEM raster representation

2.2.2 Triangulated Irregular Network (TIN)

A Triangular Irregular Network (TIN) is a vector representation of the elevation of a certain point referenced to a given level. The basic requirements for building TINs are 1) Triangles are formed with the nearest neighbor points, 2) TINs are unique if the same algorithm is used with the same data points, and 3) Triangles geometry is optimal. Two ways of using the data points for creating TINs are static and dynamic approaches. The static approach includes all the data to build as an overall network. The dynamic approach allows the addition or removal of points during the triangulation process, which allow the structure to be modified without reconstructing the complete network each time. Since it satisfies all these requirements, the Delaunay triangulation is the most often used method for building TINs. The Delaunay triangulation is a dual diagram of the Voronoi Diagram (Figure 2.4). The Voronoi Diagram represents regions enclosed by an embedded series of bisectors, each located equidistant both to the point under

consideration and to its neighbors. The Delaunay triangulation is created by connecting three neighbor points, which correspond to the center points of the Voronoi regions, forming non-overlapping triangles (Li et al., 2005).

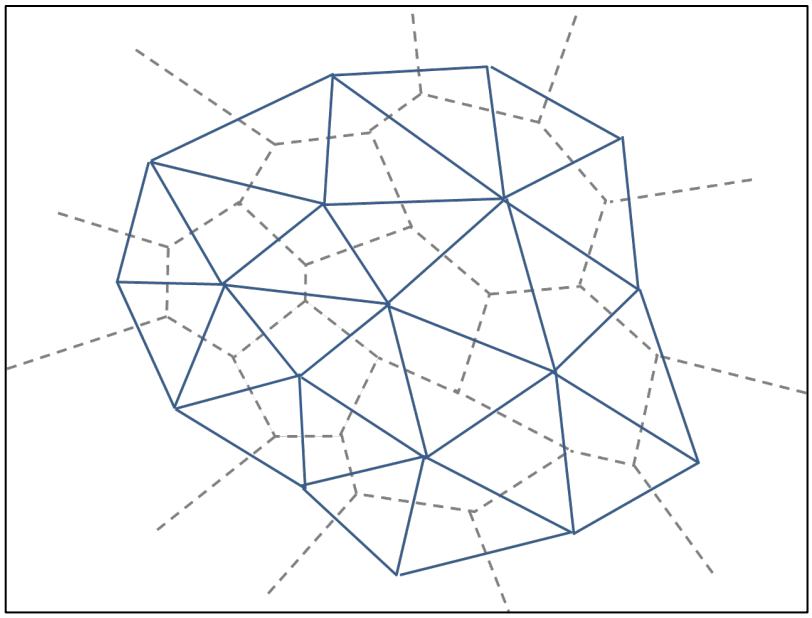

Figure 2.4: Voronoi Diagram of a point set and Delaunay triangulation (adapted from Li, 2005)

2.3 LiDAR Systems

Lasers have been used as remote sensing instruments for the last 40 years. The technological advances in last decades have made lasers more reliable and with higher resolution. Therefore, remote sensing laser-scanning systems, also known as Light Detection Ranging (LiDAR) systems, have become an essential operating tool for remote sensing, photogrammetry, and mapping. LiDAR systems are active complex remote systems that consist of 1) a laser range finder that consists of a laser emitter and a laser pulse receiver system, 2) a computer system that controls the data acquired, 3) a storage medium, 4) cameras, 5) a GP that determines the system's position and orientation, and

6) an inertial navigation system. LiDAR systems send off electromagnetic energy and register the pulse of the energy scattered back from the terrain surface or object on the terrain surface (Li et al., 2005). The receiver measures the travel time of the pulse from its launch to its return. Since the pulse travels at the speed of light and the receiver measures the travel time; the distance is obtained of the object from which the pulse reflected back. The X, Y, and Z coordinates for each point registered by each pulse is estimated with the assistance of the computer system, storage medium, scanner, and GPS. As a result, LiDAR systems provide high-resolution point clouds of the elements in the topography of a region (Jaboyedoff et al., 2010).

2.3.1 Point Cloud to DTM

The point clouds provided by LiDAR systems are large volumes of elevation data collected by the pulses emitted. The processing of this data is a complex procedure that aims to 1) filter the points, 2) classify the points, and 3) generate the elevation model (e.g. DEM raster or TIN). The point filtration removes noise points that are not needed to generate the model. The classification of the points requires finding and categorizing specific structures. Table 2.1 shows the general classification codes defined by the American Society of Photogrammetry and Remote Sensing (ASPRS, 2013).

Table 2.1: ASPRS Standard LIDAR Point Classes (2013)

Classification Value	Meaning
0	Created, never classified
1	Unclassified
2	Ground
3	Low Vegetation
4	Medium Vegetation
5	High Vegetation
6	Building

Table 2.1: Continue

Classification Value	Meaning
7	Low Point ("low noise")
8	Model Key point (mass point)
9	Water
10	Reserved for ASPRS Definition
11	Reserved for ASPRS Definition
12	Overlap points
13	Reserved for ASPRS Definition

2.3.2 Airborne and Ground-based LiDAR

There are two types of LiDAR systems, which are described as follows:

Airborne LiDAR

Airborne LiDAR is a laser scanning system installed in an aircraft or a helicopter. The number of points per second collected by an Airborne LiDAR system ranges from a few hundreds and thousands. The two types of Airborne LiDAR sensors are 1) topographic, and 2) bathymetric. The topographic sensor is used to generate surface models for applications such as hydrology, geomorphology, and urban planning. Figure 2.5 shows a graphic representation of an Airborne LiDAR system with a topographic sensor, which returns pulses of bare earth, buildings, vegetation, etc (ArcGIS Resources 2013).

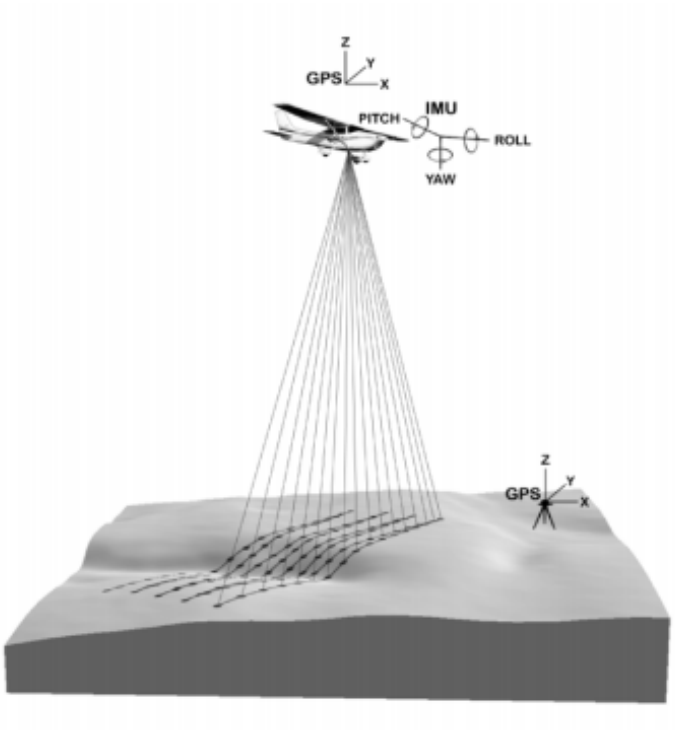

Figure 2.5: Airborne LiDAR system with topographic sensor (Andersen et al., 2006)

The bathymetric sensor is used to collect ground elevation and water depth data. As Figure 2.6 shows, the regular infrared laser is reflected back to the bathymetric LiDAR sensor from the ground or water surface, while an additional green laser travels through the water column. The results from the two pulses determine the water depth and the surface water elevation. Bathymetric LiDAR sensors are used to detect objects on the ocean floor near coastlines, harbors, offshore oil platforms, etc (ArcGIS Resources 2013).

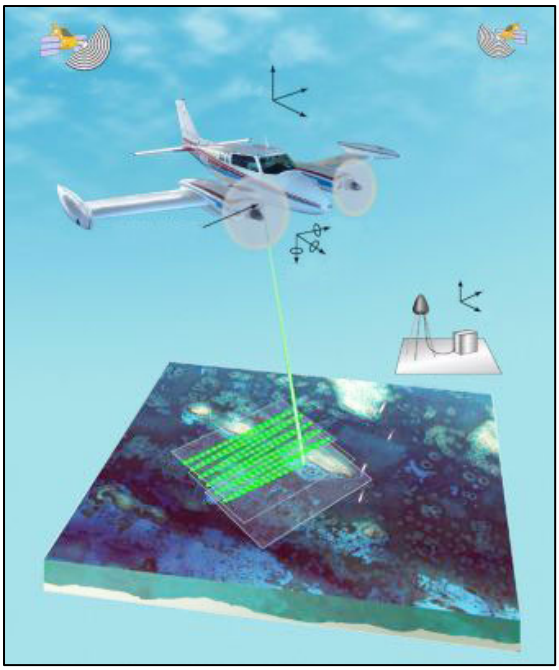

Figure 2.6: Airborne LiDAR system with bathymetric sensor (USGS, 2007)

Ground-based LiDAR

Ground-based LiDAR systems are laser-scanning systems at ground level. According to information provided during a live demonstration in October 2013 by Mandli Communications, a Ground-based LiDAR provider, the number of points per second collected by Ground-based LiDAR systems is around 1 million. The data collected with these systems helps in assessing highway conditions, building 3-D city models, planning rail maintenance, managing utility assets, etc. Ground-based LiDAR systems use two techniques for collecting data: static and mobile. The static technique is used from a fixed location with the LiDAR system usually mounted on a portable tripod collecting point clouds. This technique obtains data on building interiors and exteriors, mines, archeological sites, etc. In the mobile technique, the system is mounted on a moving vehicle, and is used for road infrastructure analyses, urban planning, asset management and smart grid implementation, bridges, vertical and horizontal clearance

estimation, etc. Figure 2.7 shows a point cloud generated by Mandli Communications with ground based LiDAR data.

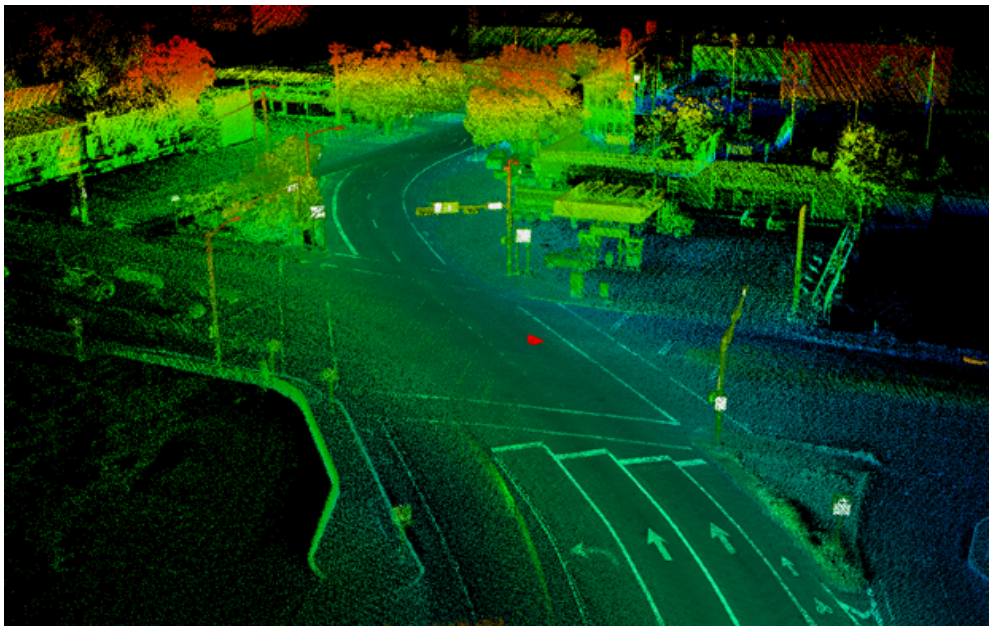

Figure 2.7: Point cloud generated by Mandli Communications with Ground-based LiDAR data

2.4 Stormwater Management in Urban Areas

Population growth in urban areas has increased in the last decades and is projected to continue increasing. This urban growth has modified the characteristics of the original land and consequently the local hydrologic processes. A major modification is the elimination of first order streams caused by altering the hydraulic characteristics of small watersheds (Davis 2005). Figure 2.8 is a graphic representation of the changes in hydrological pathways as a consequence of land development. As Figure 2.8 shows, high impervious materials replace for vegetation in post-development regions, which causes an increase in the peak flow and surface runoff, and a decrease in shallow and deep infiltration. Furthermore, the canopy interception decreases causing a lower percent of

evapotranspiration than in pre-development regions. The implementation of appropriate stormwater management systems is essential to prevent and mitigate the impacts of floods caused by the increase in surface runoff in urban areas. The fundamental principles of stormwater management systems are to 1) remove water from the site as quickly and efficiently as possible by the construction of stormwater sewer systems, and/or 2) infiltrate the stormwater to the soil and if possible recharge the aquifers by the implementation of greenroofs, rainbarrels, streetside raingardens, porous paving, etc.

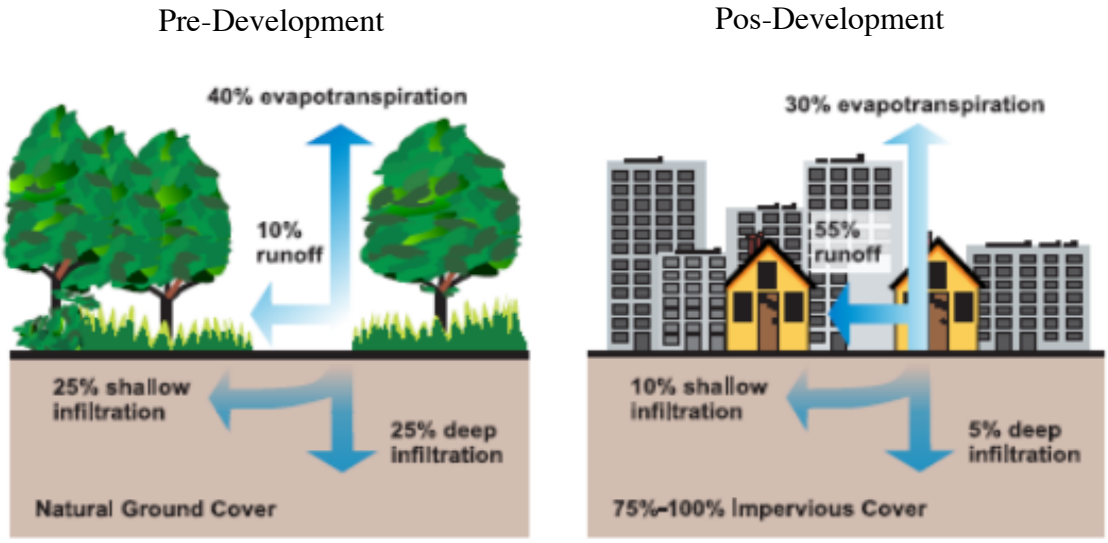

Figure 2.8: Change in hydrological pathways (EPA, 2003)

2.4.1 Stormwater sewer systems

Urban drainage systems consist of location and transfer elements. The location elements are sites where the water is stored, manipulated, and altered by human processes; for example, water treatment plants, waste water treatment plants, and water storage. The transfer elements are the features that connect the location elements; for example, pipelines, streets, and channels. In particular, a stormwater sewer system

(Figure 2.9) is a network of pipes used to transport stormwater runoff in cities to a receiving water body as quickly as possible (Chow et al., 1998). Urban stormwater sewer systems consist of minor and mayor systems. A minor system is designed for regular storm drainage and includes outfalls, curb inlets, junctions, manholes, gutters, ditches, culverts, and storm pipes. A mayor system is designed for emergency flows and includes streets, floodways, and flood fringe areas (Mays, 2001).

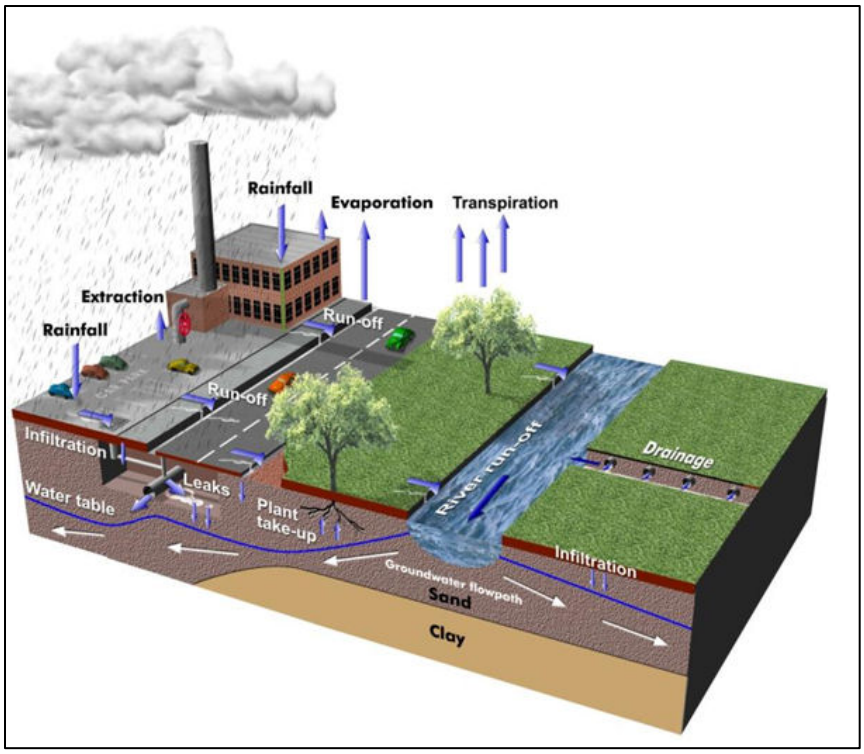

Figure 2.9: Typical Stormwater Sewer System (British Geological Survey 2014)

2.4.2 Modeling Stormwater Sewer Systems

The most important components of urban stormwater sewer systems are pipelines (Mays, 2001). In modeling these systems it is essential to take into consideration the diameters, slopes, and invert elevations for all pipes in the system (Chow et al., 1988).

The rational method is employed for modeling and predicting the runoff in these systems. This method is based on the direct relationship between rainfall and runoff in a catchment and is expressed by the following equation:

$$Q = C\ i\ A$$

where Q is the peak discharge in $acre\frac{inch}{hour}$ (1cfs = 1.008 $acre\frac{inch}{hour}$), C is the runoff coefficient, i is the rainfall intensity in inches per hour ($\frac{inch}{hour}$), and A is the drainage area in $acre$. The drainage area or catchment is traditionally determined from topographic maps, contours, or field surveys. The rational method is based on the idea that if a rainfall of a certain intensity begins suddenly and continues incessantly; the runoff rate will increase until the time of concentration, t_c (Chow et al., 1988). The time of concentration is the time it takes the water to flow from the farthest point of a watershed to the watershed outlet.

As stated in the 2013 Drainage Criteria Manual of the City of Austin, the basic assumptions associated with this method are as follows:

1. The time of concentration and the storm duration are equal.
2. The estimated peak runoff rate at the design point is a function of the average rainfall rate over the storm duration.
3. The return period of the estimated peak flow is equal to that for the storm event analyzed.
4. The runoff coefficient does not vary during a storm event.
5. The rainfall intensity is constant during a storm event and is distributed uniformly along the basin.
6. The maximum discharge rate at the design point occurs when the whole area above it contributes with the flow.

The least precise variable in this method is the runoff coefficient that represents the relationship between peak runoff and the rainfall rate for the drainage basin. This variable depends on the type of soil, vegetation, ground slope, and impervious condition of the drainage area (Chow et al., 1988). Table 2.2, from the 2013 Drainage Criteria Manual 2013 of the City of Austin, shows the runoff coefficients for several return periods and different surface characteristics.

Table 2.2: Rational Method Runoff Coefficients For Composite Analysis (Drainage Criteria Manual of the City of Austin 2013)

Character of Surface	**Return Period**						
	2 Years	**5 Years**	**10 Years**	**25 Years**	**50 Years**	**100 Years**	**500 Years**
DEVELOPED							
Asphaltic	0.73	0.77	0.81	0.86	0.90	0.95	1.00
Concrete	0.75	0.80	0.83	0.88	0.92	0.97	1.00
Grass Areas (Lawns, Parks, etc.)							
Poor Condition*							
Flat, 0-2%	0.32	0.34	0.37	0.40	0.44	0.47	0.58
Average, 2-7%	0.37	0.40	0.43	0.46	0.49	0.53	0.61
Steep, over 7%	0.40	0.43	0.45	0.49	0.52	0.55	0.62
Fair Condition**							
Flat, 0-2%	0.25	0.28	0.30	0.34	0.37	0.41	0.53
Average, 2-7%	0.33	0.36	0.38	0.42	0.45	0.49	0.58
Steep, over 7%	0.37	0.40	0.42	0.46	0.49	0.53	0.60
Good Condition***							
Flat, 0-2%	0.21	0.23	0.25	0.29	0.32	0.36	0.49
Average, 2-7%	0.29	0.32	0.35	0.39	0.42	0.46	0.56
Steep, over 7%	0.34	0.37	0.40	0.44	0.47	0.51	0.58

Table 2.2: Continue

Character of Surface	Return Period						
	2 Years	**5 Years**	**10 Years**	**25 Years**	**50 Years**	**100 Years**	**500 Years**
UNDEVELOPED							
Cultivated							
Flat, 0-2%	0.31	0.34	0.36	0.4	0.43	0.47	0.57
Average, 2-7%	0.35	0.38	0.41	0.44	0.48	0.51	0.6
Steep, over 7%	0.39	0.42	0.44	0.48	0.51	0.54	0.61
Pasture/Range							
Flat, 0-2%	0.25	0.28	0.3	0.34	0.37	0.41	0.53
Average, 2-7%	0.33	0.36	0.38	0.42	0.45	0.49	0.58
Steep, over 7%	0.37	0.4	0.42	0.46	0.49	0.53	0.6

The rainfall intensity variable is selected based on the design rainfall duration and design frequency occurrence. The rainfall duration is equal to the time of concentration, which is the sum of 1) sheet flow travel time, 2) shallow concentrated flow travel time, and 3) storm drain flow travel time. The frequency occurrence or the return period is a statistical estimate of the likelihood of an event to occur over a period of time. The rainfall intensity used in the rational method can be estimated from intensity-duration-frequency curves (IDF), which are the relationship between rainfall intensity, duration, and return period appropriate for the region analyzed. Table 2.3 shows an example of an IDF table for Austin and Travis County (Drainage Criteria Manual of the City of Austin 2013).

Table 2.3: Intensity-Duration-Frequency Table for Austin and Travis County (Drainage Criteria Manual of the City of Austin, 2013)

Intensity of Precipitation (inches per hour)									
Recurrence Interval (year)	**Duration (min or hr)**								
	5 min	**15 min**	**30 min**	**1-hr**	**2-hr**	**3-hr**	**6-hr**	**12-hr**	**24-hr**
2	5.76	3.92	2.64	1.72	1.08	0.773	0.445	0.255	0.143
5	7.39	5.04	3.42	2.28	1.45	1.04	0.593	0.339	0.208
10	8.57	5.88	3.96	2.68	1.71	1.24	0.702	0.401	0.254
25	10.1	7.04	4.72	3.28	2.1	1.52	0.857	0.492	0.318
50	11.2	8.04	5.36	3.79	2.44	1.76	0.99	0.572	0.37
100	12.5	9.16	6.08	4.37	2.83	2.04	1.14	0.663	0.424
250	14.5	10.9	7.14	5.26	3.43	2.46	1.37	0.806	0.501
500	15.9	12.4	8.04	6.06	3.97	2.84	1.58	0.934	0.564

Traditional methodologies use low-resolution DEM raster files and/or topographic maps from field measurements to characterize the elements of stormwater sewer systems. The main flaws of traditional methods are the lack of vertical accuracy of low-resolution DEM raster files (Ritchie, 2009), while field surveys are time consuming and do not give a continuous representation of elevation points in space. These methods also use specialized software models such as StormCAD, SWMM, or Hydra, and can integrate GIS, and LiDAR data to build dynamic and precise models. These tools will allow us estimate accurately the ground elevation, identify obstructions on the ground, distinguish the water flowpath, and digitize more precisely the drainage areas.

Chapter 3: Methodology

3.1 Processing LiDAR Data in ArcGIS

LiDAR data can be processed within ArcGIS as LAS files. The three formats to manage, work, and process these data in ArcGIS are 1) LAS dataset, which helps to visualize and make updates to the LAS files; 2) Mosaic dataset that are used to create a raster; and 3) Terrain dataset, which are used to represent the terrain as TINs. The 4 LAS files used in this thesis were collected by Airborne LiDAR at the main campus area and the surroundings of The University of Texas at Austin (UT); the projected coordinate system used is NAD_1983_StatePlane_Texas_Central_FIP with feet as linear unit.

3.1.1 Create LAS dataset

A LAS dataset is created using the "Create a LAS dataset" tool of the Data Management toolbox of ArcMap, which requires the LAS files as inputs and the name and place of storage of the output LAS dataset. This LAS dataset helps to visualize the LiDAR data in 2-D and 3-D, and to make changes in the classification of the data. Figure 3.1, shows a 2-D and 3-D view of the LiDAR dataset of UT's main building block

2-D Perspective

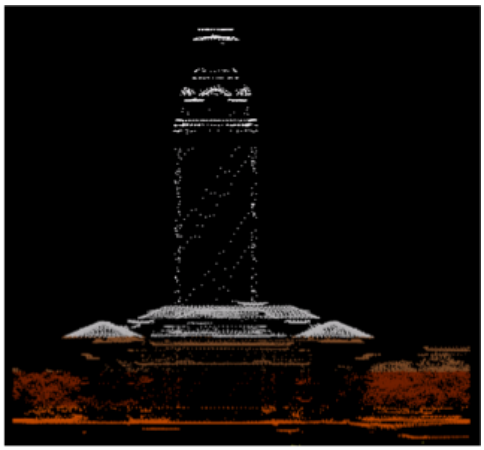

3-D Perspective

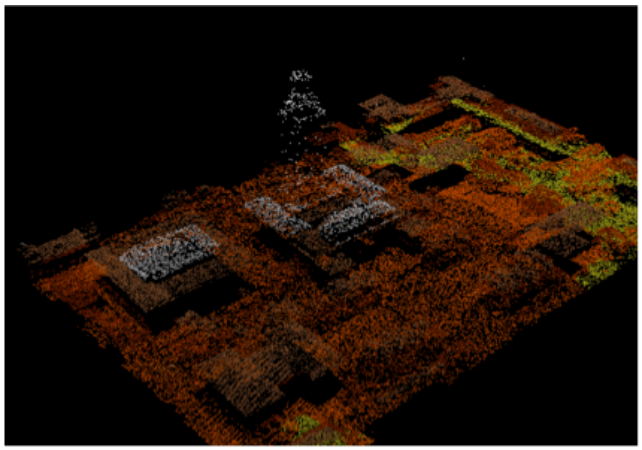

Figure 3.1: 2-D and 3-D perspective of UT's main building LiDAR dataset created with Airborne LiDAR

3.1.2 Point File Toolbox

The data or points collected from a LiDAR system have to be analyzed before creating a DTM. Therefore, it is needed to generate the statistics of the LAS files, which are obtained using the "Point File Information" tool of the 3-D Analyst toolbox of ArcMap. The inputs required for this tool are the LAS files, and the data required for the output is the name and location of the feature class this tool generates. A feature class is a homogeneous collection of geographic features with the same spatial representation (points, polylines, or polygons) and the same attribute columns that are stored inside a geodatabase; which is a storage framework that combines the spatial data and the data repository. Table 3.1 shows an attribute table of the feature class created by running the Point File Information tool with the LAS files of UT's main campus area. As can be seen in Table 3.1, the statistics obtained from this tool are the point count, point spacing, the minimum and maximum elevation, shape length, and shape area of each of the LAS files.

Table 3.1: Attribute table of the feature classes generated after running ArcGIS' Point File Information tool for the LAS files of UT's main campus area

Table

PointFileInfoThesis

OID *	Shape *	FileName	Pt_Count	Pt_Spacing	Z_Min	Z_Max	Shape_Length	Shape_Area
1	Polygon	AUSTIN_EAST-SWA3.las	14382400	1.434716	336.83	2181	21807.920044	29604888.456622
2	Polygon	AUSTIN_EAST-SWA4.las	15814570	1.368368	474.14	1996.88	21810.300049	29611704.446285
3	Polygon	AUSTIN_EAST-SWC1.las	13587160	1.471301	385.04	1033.4	21732.540039	29412487.618469
4	Polygon	AUSTIN_EAST-SWC2.las	14467808	1.425804	447.94	1937.72	21732.160034	29411836.735916

1 (0 out of 4 Selected)

PointFileInfoThesis

3.1.3 LAS to Multipoint

The point classification of the LAS files follows the standards defined by the 2013 ASPRS report (Table 2.1). The points needed for the purpose of this thesis are the

classified as ground (2) and buildings (6). The "LAS to Multipoint" tool of the 3-D analyst toolbox of ArcMap generates a multipoint feature class. Multipoint feature classes are features composed of more than one point used to manage clusters of points. The inputs of this tool are the LAS files, and the output needed is the name and location of the feature class this tool generates. Furthermore, this tool requires the average point spacing obtained from the Point File Information tool, and specify the point classes needed. Figure 3.2 shows the ground and buildings multipoints generated from UT's main campus LAS files.

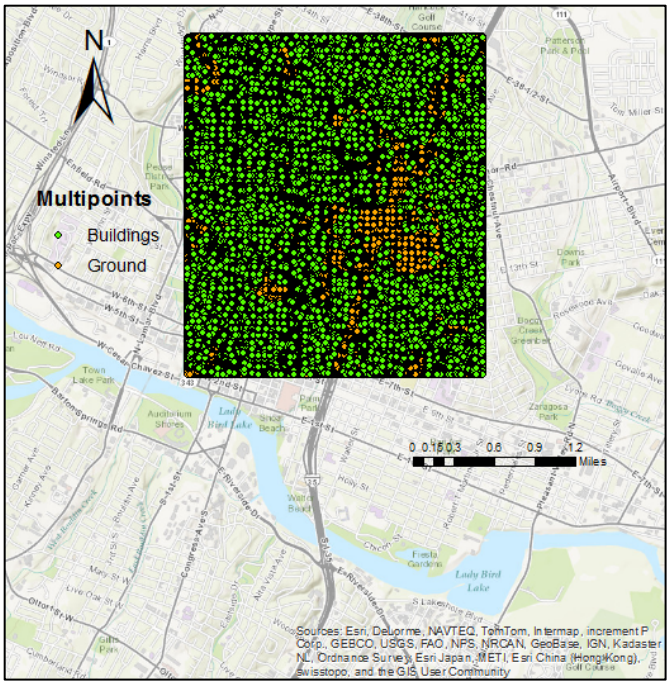

Figure 3.2: Ground and buildings multipoints generated from UT's main campus LAS files

3.1.4 Create Tin

The multipoints generated from the LAS to Multipoint tool are used to build the TIN of UT's main campus area. The "Create TIN" tool of the 3-D Analyst toolbox of

ArcMap is used to build this TIN. Furthermore, a polygon feature class is used as breakline to limit the TIN to the extent of UT's main campus and surrounding area. The inputs feature classes needed for running this tool includes 1) the ground and buildings multipoints with Height Field specified as Shape.Z, Surface Type as Mass Points, and the Tag Field as none; and 2) the polygon feature class with Height Field specified as none, Surface Type as soft clip, and the Tag Field as none. The output requirement is the name and storage location of the TIN.

The TIN generated is heavy and oversampled and is possible to remove redundant points or nodes. The "Decimate Tin Node" tool is a 3-D Analyst tool of ArcMap that creates a new TIN by removing unnecessary nodes without altering the original resolution. The inputs of the Decimate Tin Node tool are the original TIN and Z tolerance needed to maintain the accuracy after the interpolation, while the output requirement is the name and storage location of the new TIN. The TIN generated from this tool also contains high-resolution elevation data of UT's main campus, which is essential for analyze precisely current and future infrastructure conditions. This elevation data is ready for analyzing the hydrology and stormwater infrastructure of UT's main campus. Figure 3.3 and Figure 3.4 show the TIN generated of UT's main campus and surrounding area in 2-D and 3-D respectively.

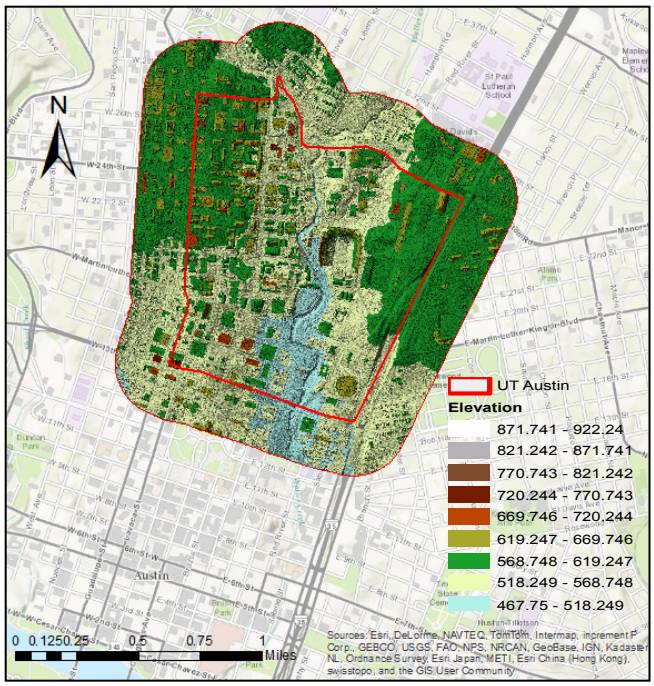

Figure 3.3: 2-D view of the TIN created based on Airborne LiDAR data of UT's main campus and surrounding area

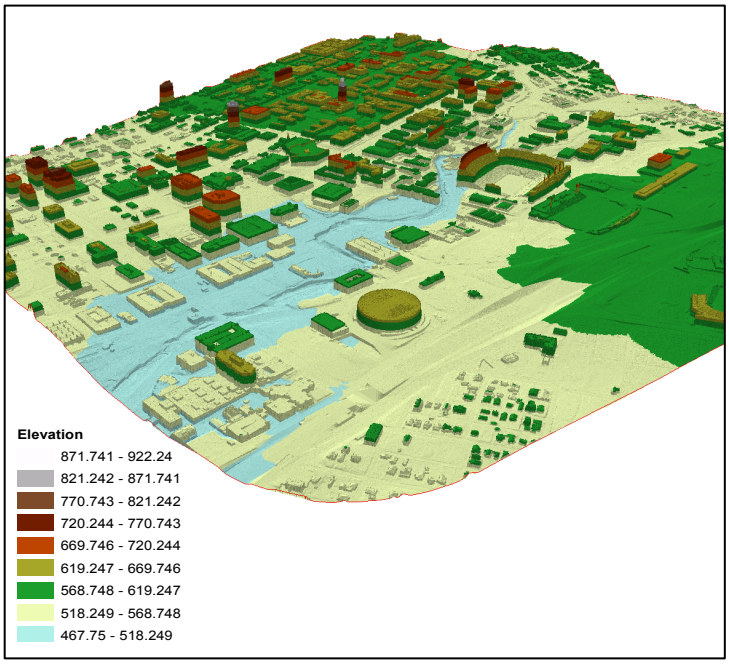

Figure 3.4: 3-D view of the TIN created based on Airborne LiDAR data of UT's main campus and surrounding area

Figure 3.5 shows a zoom-in view of the TIN in 3-D that helps to visualize the nodes and edges that comprise the TIN.

View of face elevation with graduated color ramp of the TIN

View of nodes and edges that form the TIN

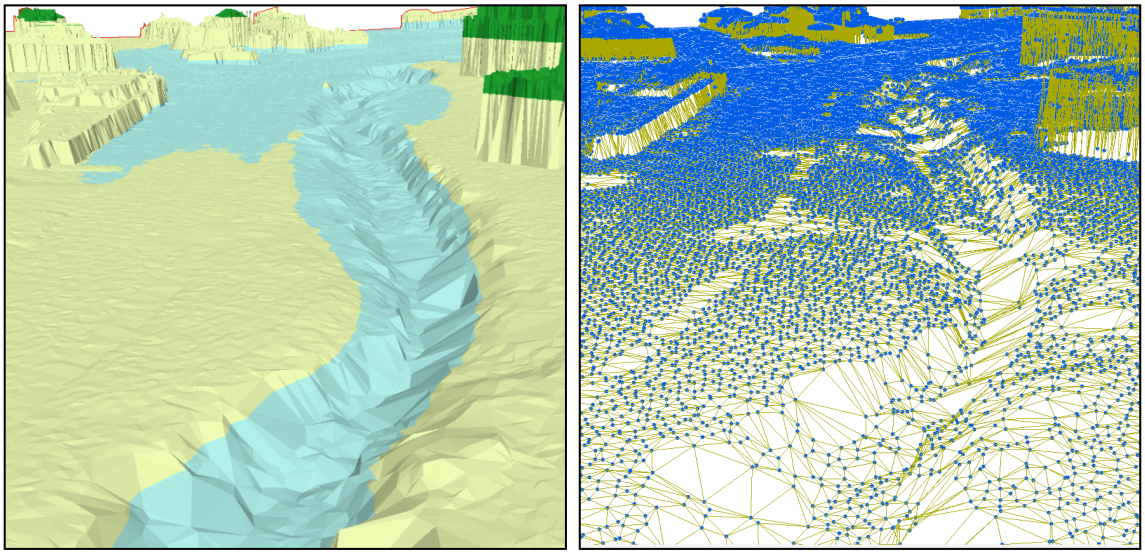

Figure 3.5: Zoom-in view of TIN in 3-D at Waller Creek at the north area of UT´s main campus

3.1.5 Tin to Raster

The TIN created is used to generate a DEM raster through interpolation with the "TIN to Raster" tool of the 3-D Analyst toolbox of ArcMap, which requires the TIN as input. This tool allows 1) changing the interpolation method (linear or natural neighbors), 2) sampling distance of the raster cells, and 3) changing the output data type (float or integer). The output requirement is the name and storage location of the DEM raster. Figure 3.6 and Figure 3.7 show UT's main campus DEM raster in 2-D and 3-D respectively.

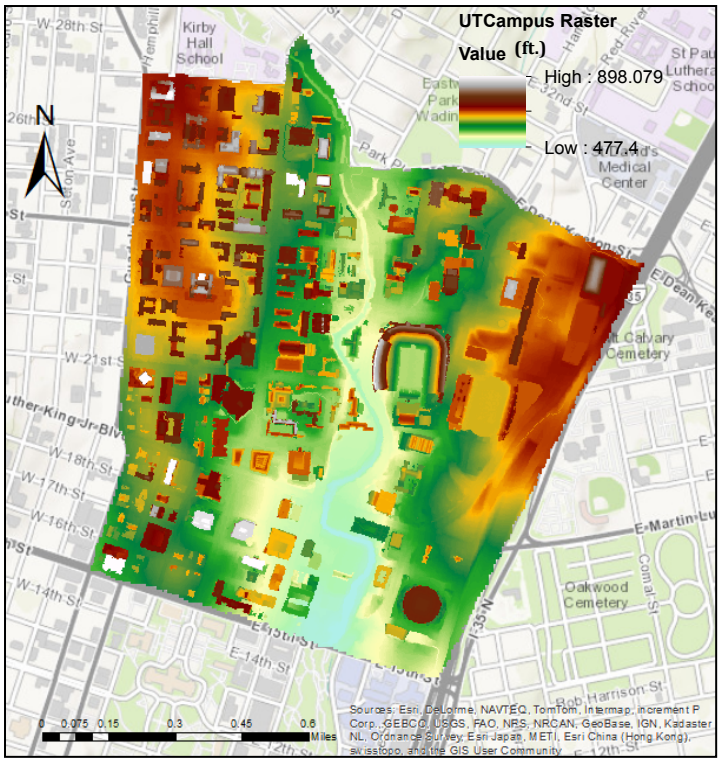

Figure 3.6: 2-D view of UT's main campus DEM raster (ground and buildings)

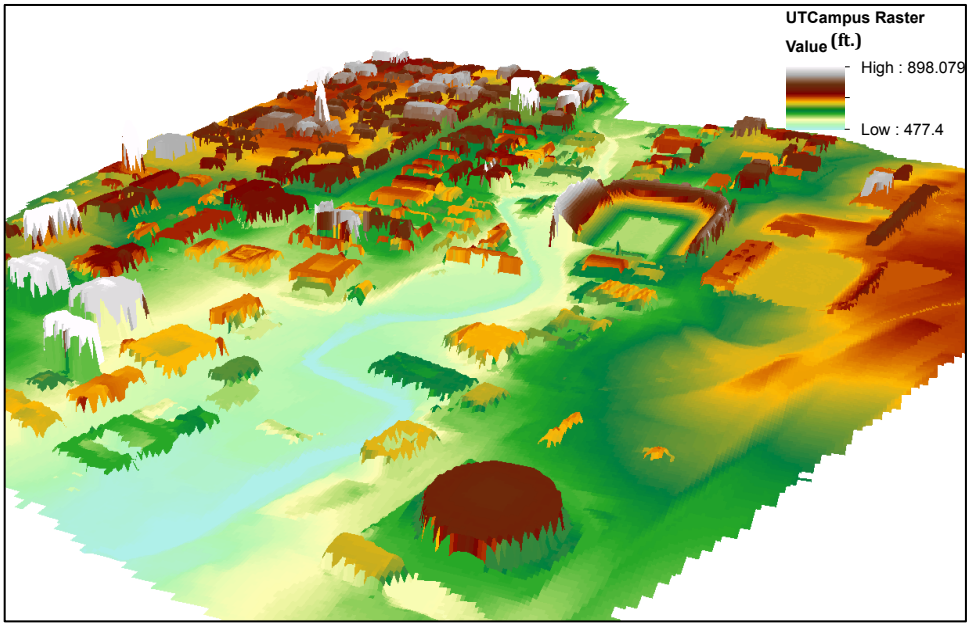

Figure 3.7: 3-D view of UT's main campus DEM raster (ground and buildings)

3.2 Modeling Stormwater Sewer Systems using LiDAR Data

The model for evaluating the current conditions of a stormwater sewer system consists on assessing the system's elements for different storm scenarios. The system's elements are digitized and characterized in ArcMap with data from the TIN, drainage manuals, and local authorities. After the system is digitized, StormCAD (a specialized software) is used to evaluate the system for storm scenarios with 4 return periods (2, 10, 25 and 100 years) in the northwest area of UT's main campus. Figure 3.8 shows the location of the area analyzed.

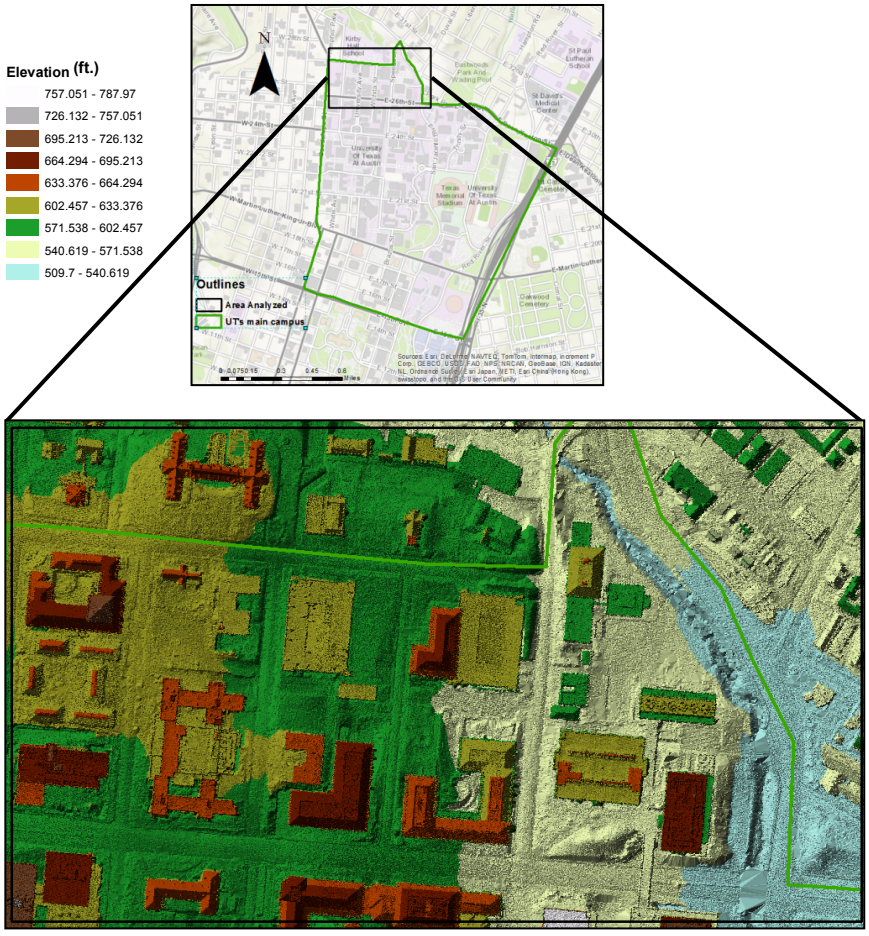

Figure 3.8: Northwestern area of UT's main campus used for modeling the stormwater sewer system

3.2.1 Digitizing Stormwater Sewer Systems in ArcMap

The digitization and characterization of the stormwater sewer system's elements in ArcMap comprise the generation of feature classes representing 1) Manholes as points, 2) Curb Inlets as points, 3) Joints as points, 4) Outfalls as points, 5) Drainage Pipelines as polylines, and 6) Catchments as polygons. The steps for digitizing these elements are as follows:

1. Import the CAD files of UT's stormwater sewer system. This step is done with the "Add CAD files" tool of the Conversion toolbox of ArcMap. It is necessary to have all the data with the same projected coordinate system, which is NAD_1983_StatePlane_Texas_Central_FIP with feet as linear unit. Figure 3.9 shows the CAD files of UT's stormwater sewer system imported to ArcMap. The features imported from the CAD files are useful as guideline to create and define certain characteristics of the feature classes needed to create the model of the stormwater sewer system.

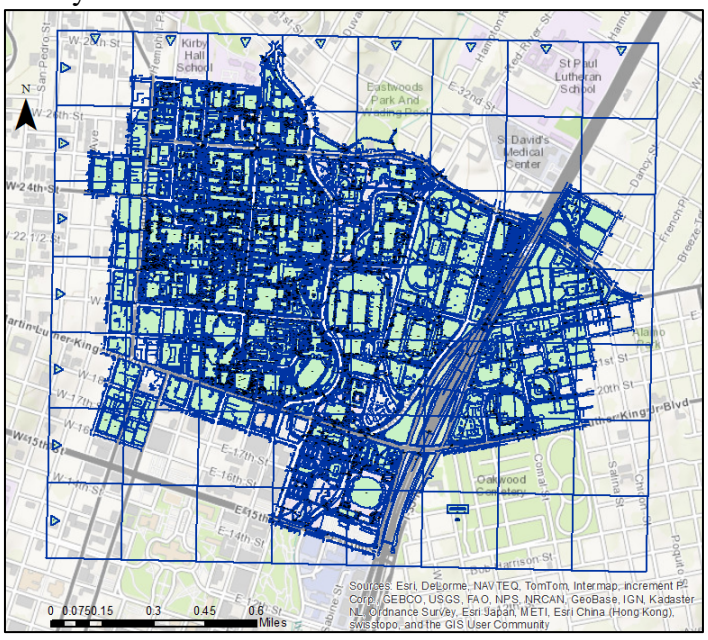

Figure 3.9: CAD files of UT's stormwater sewer system imported to ArcMap

2. Create a file geodatabase and the features classes to model the stormwater sewer system. A geodatabase is created using the "Create File Geodatabase" tool of the Data Management toolbox of ArcMap, which requires as input the name and storage location of the geodatabase. This geodatabase is used to store all the feature classes that are generated for characterizing and analyzing the stormwater sewer system. The feature classes are created using the "Create Feature Class" tool of the Data Management toolbox of ArcMap. This tool requires the location of the geodatabase used to storage the feature classes, name, geometry type (polyline, polygon, point, or multipoint), and coordinate system of the feature class (NAD_1983_StatePlane_Texas_Central_ FIP with feet as linear unit). The feature classes created are shown in Table 3.2.

Table 3.2: List of feature classes created for modeling the stormwater sewer system

Feature Class	Description	Geometry Type
Manholes	Maintenance hole of the system	Point
Curb Inlets	Inlet of the system located adjacent to the curb	Point
Joints	Point were pipelines converge or deviate	Point
Outfalls	Discharge outlet of the system	Point
Drainage Pipelines	Pipes that transport water in the system	Polyline
Catchments	Drainage areas of inlets	Polygon
Time of concentration flowpaths	Longest flowpath water take to cross a catchment	Polyline
Building footprints	Area occupied by buildings	Polygon
Sidewalks, parking lots and streets	Impervious area of the area studied	Polygon

3. Edit the feature classes to digitize the elements required for modeling the system. The feature classes are edited using the CAD files and TIN as guidelines. As shown in Figure 3.10, the general system in the CAD files is simplified by digitizing the principal elements, which is essential to reduce the modeling computational time. On the other hand, the TIN is used for digitizing catchments, time of concentration flowpaths, buildings footprints, sidewalks, parking lots, and streets (Figure 3.11 and Figure 3.12). It is fundamental to check that 1) the catchments do not overlap or have gaps in between, and 2) the drainage pipelines starts and ends in a point feature class.

Figure 3.10: Stormwater sewer system elements simplified from CAD files

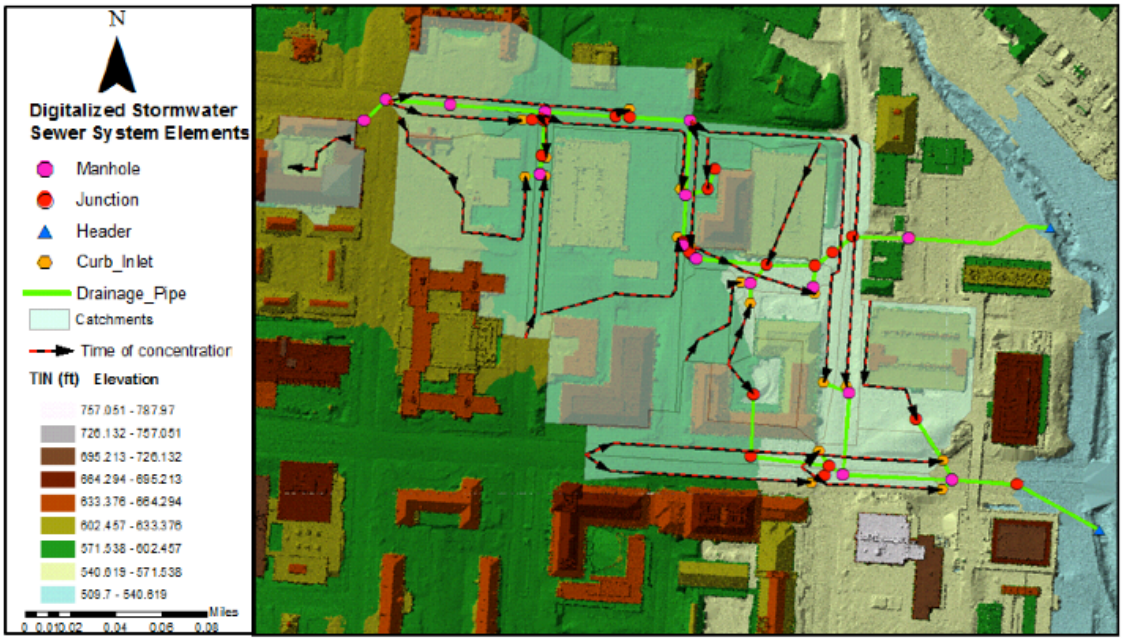

Figure 3.11: Catchments and time of concentration flowpaths digitized using the TIN

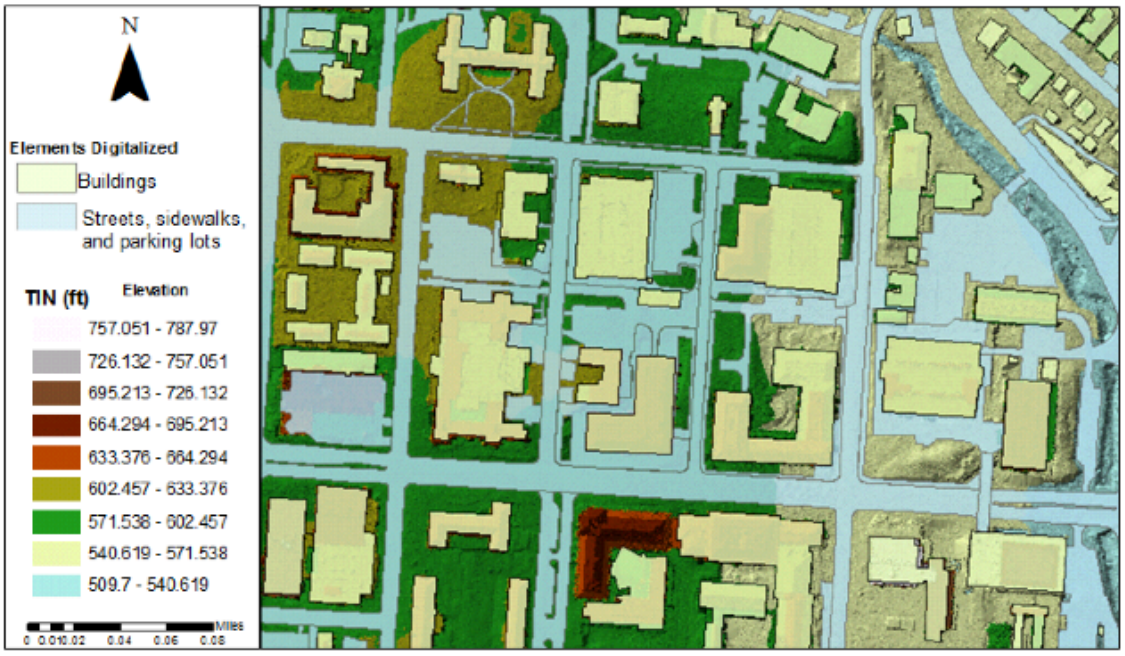

Figure 3.12: Buildings, streets, sidewalks, and parking lots digitized using TIN

4. Characterize the feature classes used to model the stormwater sewer system. The first step for characterizing the features is to assign a unique label to the manholes, curb inlets, joints, outfalls, and drainage pipelines. This is useful to identify easily each element and correlate them with their catchments, which are assigned the same unique label of their drainage feature. The methodologies employed to determine the feature classes' characteristics needed for modeling the stormwater sewer system are as follow:

   a. Manholes, curb inlets, joints, and outfalls characteristics

      i. Ground Elevation, which is obtained from the TIN data using "Add Surface Information" tool of Data Management toolbox in ArcMap.

      ii. Invert Elevation, which is obtained from field measurements. This data was provided by the City of Austin.

   b. Drainage pipelines characteristics

      The characteristics needed are the diameter, conduit type, section type, section size, and material of the pipelines. This data is obtained from the CAD files of the storm sewer system of The University of Texas at Austin

   c. Time of concentration flowpaths characteristic

      The characteristic needed is the time of concentration of each catchment. The time of concentration is estimated based on the Training Manual and the ArcMap tool created by the City of Austin (2014), which follows the methodology indicated in the Drainage Criteria Manual of the City of Austin (2013). The equation for obtaining the time of concentration in urban areas is

$$T_c = t_{t\,SF} + t_{t\,SC}$$

where T_c is the time of concentration in minutes, T_{TSF} is the travel time of the sheet flow in minutes, and T_{TSC} is the travel time of the shallow concentrated flow in minutes.

The sheet flow occurs when the travel distance of water is less than 100 ft. As stated in the Drainage Criteria Manual of the City of Austin (2013), the equation used for estimating the sheet flow travel time is

$$T_{t\,SF} = \frac{0.007(nL)^{0.8}}{P_2^{0.5}\, s^{0.4}}$$

where T_{tSF} is the sheet flow travel time (minutes), L is the length of the reach (ft), n is the manning coefficient (Table 3.3), P_2 is the depth (inches) of precipitation for a 24-hour rainfall with 2-year return period (Table 3.4), and s is the slope of the ground (ft./ft.).

Table 3.3: Manning's Coefficient for different surface descriptions (Drainage Criteria Manual of the City of Austin, 2013)

Manning's coefficient	**Surface Description**
0.015	Concrete (rough or smoothed finish)
0.016	Asphalt
0.05	Fallow (no residue)
Cultivated Soils:	
0.06	Residue Cover ≤ 20%
0.17	Residue cover > 20%
Grass:	
0.15	Short-grass prairie
0.24	Dense grasses
0.13	Range (natural)
Woods:	
0.04	Light underbrush
0.8	Dense underbrush

Table 3.4: Depth-Duration-Frequency Table for Austin and Travis County (Drainage Criteria Manual of the City of Austin, 2013)

Depth of Precipitation (in inches)									
Recurrence Interval (year)	5 min	15 min	30 min	1-hr	2-hr	3-hr	6-hr	12-hr	24-hr
2	0.48	0.98	1.32	1.72	2.16	2.32	2.67	3.06	3.44
5	0.62	1.26	1.71	2.28	2.89	3.13	3.56	4.07	4.99
10	0.71	1.47	1.98	2.68	3.42	3.71	4.21	4.81	6.1
25	0.84	1.76	2.36	3.28	4.2	4.55	5.14	5.9	7.64
50	0.94	2.01	2.68	3.79	4.88	5.28	5.94	6.86	8.87
100	1.05	2.29	3.04	4.37	5.66	6.11	6.85	7.96	10.2
250	1.21	2.73	3.57	5.26	6.86	7.38	8.24	9.67	12
500	1.33	3.11	4.02	6.06	7.94	8.51	9.47	11.2	13.5

The shallow concentrated flow occurs when the travel distance of water is greater than 100 ft. As stated in the Drainage Criteria Manual of the City of Austin (2013), the equation used for estimating the sheet flow travel time in unpaved areas is

$$T_{t\,SC} = \frac{L}{60(16.1345)(s)^{0.5}}$$

and for paved areas is

$$T_{t\,SC} = \frac{L}{60(20.3282)(s)^{0.5}}$$

where $T_{t\,SC}$ is the travel time for shallow concentrated flow (minutes), L is the length of the reach (ft), and s is the slope of the ground (ft/ft).

d. Buildings footprint characteristic

The characteristic needed for characterize the building footprint is the area of each of the buildings located in the area of study. This data is obtained in ArcMap using the Calculate Geometry tool in the attribute table of the buildings footprint feature class.

e. Sidewalk, parking lots, and streets characteristics

The characteristics needed for characterize the polygons that comprise this feature class are the area and type of material (asphalt or concrete) of each polygon. The area is obtained with ArcMap using the Calculate Geometry tool in the attribute table of this feature class, while the material is obtained from field visits and using imagery.

f. Catchments characteristics

i. Area

The area of the catchments is obtained in acres and square feet using the Calculate Geometry tool in the attribute table of the feature class in ArcMap.

ii. Time of Concentration

The time of concentration is obtained from the Time of Concentration feature class. The minimum value for the time of concentration is 5 minutes; therefore, the time of concentration used is the maximum value between the one estimated in the time of concentration feature class and 5 minutes.

iii. Rational C for all return periods

The runoff coefficient or rational C is estimated based on the Training Manual and the ArcMap tools integrated by the City of Austin (2014), which follows the procedure of the Drainage Criteria Manual of the City of Austin (2013). These tools estimate the areas of the 1) buildings; 2) sidewalks, streets, and parking lots; and 3) grass that correspond to each catchment. These areas are multiplied by the appropriate runoff coefficient shown in Table 2.2.

3.2.2 Building model in StormCAD

The feature classes needed to build the model are the manholes, curb inlets, joints, outfalls, drainage pipelines, and catchments. These features have to be exported outside the geodatabase as shapefiles to import them to StormCAD. StormCAD is the software used to evaluate the stormwater sewer system capacity. The steps to build the models are based on the StormCAD Training Manual of the City of Austin (2014) and are as follows:

1. Extract the catalog conduit from the Engineering Library of StormCAD, which includes the characteristics of the pipes in the stormwater sewer system analyzed.
2. Define the storm data from the Drainage Criteria Manual (2013) of the City of Austin (Table 2.3). Figure 3.13 shows the IDF curve and table defined in StormCAD for the 4 storm scenarios analyzed (2, 10, 25, and 100 year return period).

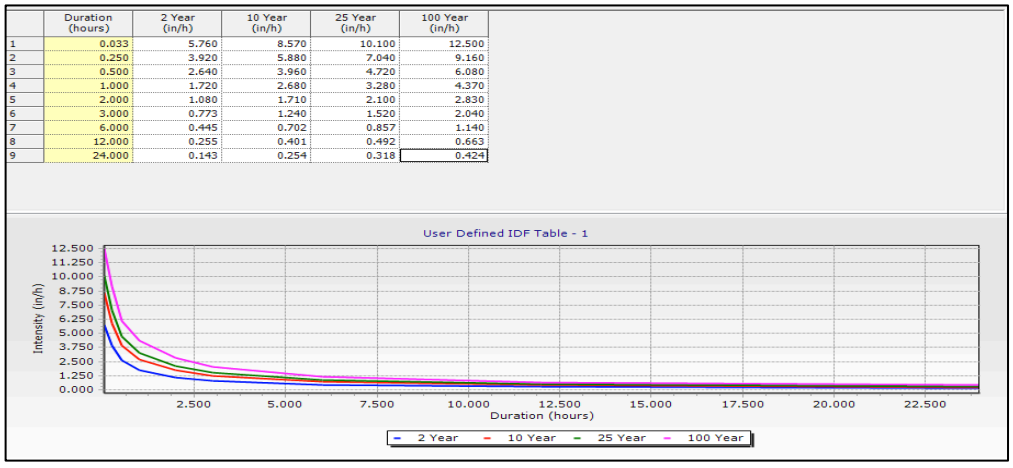

	Duration (hours)	2 Year (in/h)	10 Year (in/h)	25 Year (in/h)	100 Year (in/h)
1	0.033	5.760	8.570	10.100	12.500
2	0.250	3.920	5.880	7.040	9.160
3	0.500	2.640	3.960	4.720	6.080
4	1.000	1.720	2.680	3.280	4.370
5	2.000	1.080	1.710	2.100	2.830
6	3.000	0.773	1.240	1.520	2.040
7	6.000	0.445	0.702	0.857	1.140
8	12.000	0.255	0.401	0.492	0.663
9	24.000	0.143	0.254	0.318	0.424

Figure 3.13: IDF curve of Austin for the 4 different storm scenarios analyzed (Data used from the Drainage Criteria Manual, 2013)

3. Create the 4 alternative storm scenarios that are used to evaluate the stormwater sewer system.

4. Import the features as shapefiles. This step is done using the Model Builder wizard of StormCAD, where the data source files can be found under the Esri Shapefiles type. The shapefiles are imported in clusters of 1) points (manholes, curb inlets, joints, and outfalls), 2) polylines (drainage pipelines), and 3) polygons (catchments). The coordinate unit selected is feet and there is no need for referencing the objects automatically, which is consistent with the units and projected coordinate system used to create the shapefiles in ArcMap. The characteristics of the shapefiles have to be related with the StormCAD settings as follows:

   a. Point shapefiles

      - Manholes
        - The option "Manhole" is selected for the "Table Type" setting.
        - The "Key Fields" setting selected is the unique label assigned in ArcMap.
        - The unique label given in ArcMap is assigned the "Label" property.
        - The terrain elevation given in ArcMap is assigned the "Elevation (ground)" property and the unit selected is "feet".
        - The invert elevation given in ArcMap is assigned the "Elevation (invert)" property and the unit selected is "feet".
      - Curb Inlets.
        - The option "Catch Basin" is selected for the "Table Type" setting.
        - The "Key Fields" setting selected is the unique label assigned in ArcMap.

- The unique label given in ArcMap is assigned the “Label” property.
- The terrain elevation given in ArcMap is assigned the “Elevation (ground)” property and the unit selected is “feet”.
- The invert elevation given in ArcMap is assigned the “Elevation (invert)” property and the unit selected is “feet”.

- Joints.
  - The option “Transition” is selected for the “Table Type” setting.
  - The “Key Fields” setting selected is the unique label assigned in ArcMap.
  - The unique label given in ArcMap is assigned the “Label” property.
  - The terrain elevation given in ArcMap is assigned the “Elevation (ground)” property and the unit selected is “feet”.
  - The invert elevation given in ArcMap is assigned the “Elevation (invert)” property and the unit selected is “feet”.
- Outfalls.
  - The option “Outfall” is selected for the “Table Type” setting.
  - The “Key Fields” setting selected is the unique label assigned in ArcMap.
  - The unique label given in ArcMap is assigned the “Label” property.
  - The terrain elevation given in ArcMap is assigned the “Elevation (ground)” property and the unit selected is “feet”.
  - The invert elevation given in ArcMap is assigned the “Elevation (invert)” property and the unit selected is “feet”.

b. Polyline shapefile

The Drainage Pipelines shapefile is assigned the following settings:

- The option “Conduit” is selected for the “Table Type” setting.
- The “Key Fields” setting selected is the unique label assigned in ArcMap.
- The unique label given in ArcMap is assigned the “Label” property.
- The diameter of the pipelines registered in ArcMap is assigned the “Diameter” property and the unit selected is “inches”.
- The conduit type given in ArcMap is assigned the “Conduit Type (label)” property.
- The section type given in ArcMap is assigned the “Section Type (label)” property.
- The section size given in ArcMap is assigned the “Section Size (Catalog Conduit) (Label)” property.
- The conduit material given in ArcMap is assigned the “Material” property.

c. Polygons

The Catchments shapefile is assigned the following settings:

- The option “Catchment” is selected for the “Table Type” setting.
- The “Key Fields” setting selected is the unique label assigned in ArcMap.
- The unique label given in ArcMap is assigned the “Outfall Element (Label)” property.
- The area in acres obtained in ArcMap is assigned the “Area” property and the unit selected is “acres”.
- The time of concentration estimated in ArcMap is assigned the “Time of Concentration” property and the unit selected is “minutes”.

- The runoff coefficient for a 2-year return period estimated in ArcMap is assigned the “Rational C” property.

5. Synchronize the drawings in StormCAD. The shapefiles are drawn after importing and closing the model builder for the 2-year return period scenario. It is necessary to 1) change the scenario option to the 10-year storm scenario, 2) open the model builder, 3) change the Rational C property for the runoff coefficient of the 10-year storm event, 4) synchronize the drawing, and 5) repeat this procedure for the 25 and 100 year scenarios. Figure 3.13 shows the sketch drawn with the shapefiles imported to StormCAD.

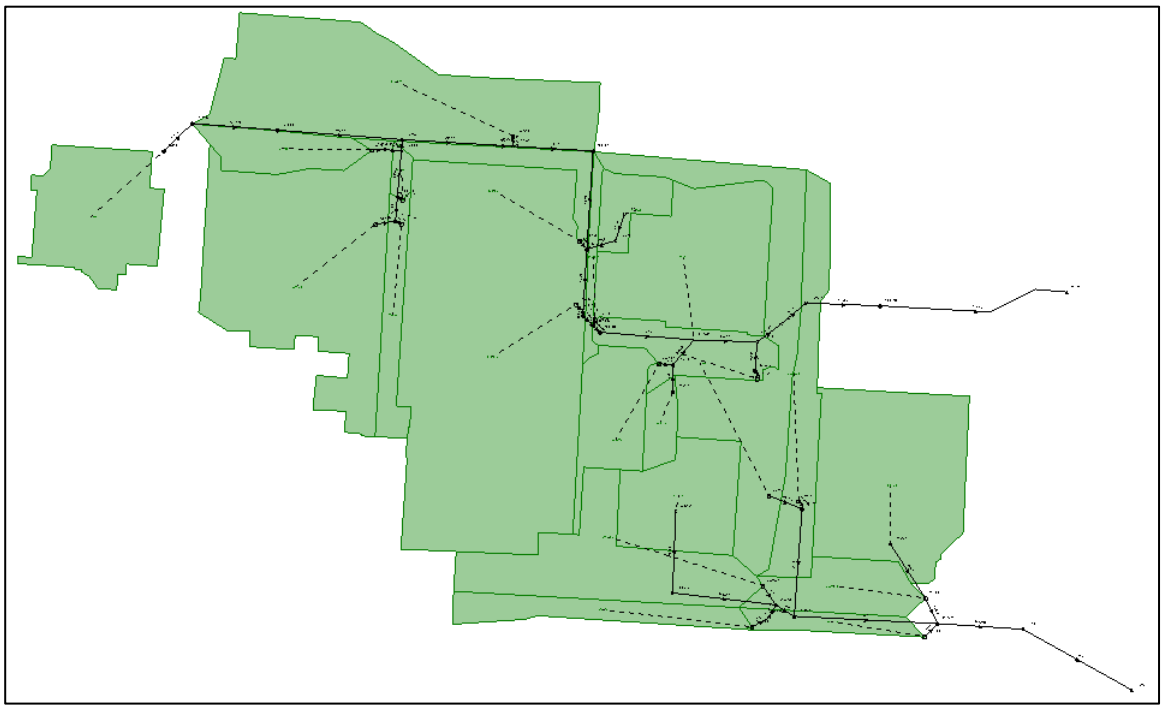

Figure 3.13: Sketch in StormCAD of the elements of the stormwater sewer system analyzed

The symbols used by StormCAD to illustrate the shapefiles are 1) green polygons for catchments, 2) lines for pipelines, 3) ⊙ symbols for manholes, 4) □ symbols for catch basins or inlets, 5) O symbols for junctions, and 6) △ symbols for outfalls.

6. Establish outfall conditions for all the storm scenarios. The outfalls boundary condition for all the scenarios is selected as water surface elevation, which means that the stream conditions at the discharge of the system affects the hydraulic response of the stormwater sewer system.

7. Add gutters from the on-grade inlets to the in-sag inlets. The gutters are added directly in StormCAD following the direction of the water that is captured by the previous inlet. As shown in Figure 3.14, it is useful to add an imagery picture as background to take into consideration the flow direction and street obstructions.

Figure 3.14: Gutter drawn in StormCAD with imagery of the area analyzed as background

8. Define the headloss coefficient or k-value for the manholes, joints and curb inlets. As suggested in the Training Manual of the City of Austin (2014), which is based on the City of Austin Drainage Criteria Manual (2013), the headloss coefficients defined for the manholes joints, and curb inlets are as follows:
    a. Inlets at the end of the line are defined by the standard method with a headloss coefficient of 1.25
    b. Inlets in the middle of the line, manholes, and joints are defined by the HEC-22 Energy method with a flat HEC-22 benching method.

3.2.3 Running Model

The model built has to be validated before running it for each storm scenario analyzed (2, 10, 25, and 100 year return period). According to StormCAD Users Guide (2013), the steps followed by StormCAD when running the model are 1) generate surface loads and perform the inlets computation, 2) route intercepted loads downstream through the pipelines, and 3) compute headlosses upstream through the pipelines. The pipe profiles have an effect on travel times, and the rational loads affect the hydraulic characteristics of the pipes; therefore, the calculation process used by StormCAD is iterative until convergence is reached or the maximum number of iterations is computed.

Chapter 4: Results

4.1 TIN AND DEM RASTER PROFILES

The TIN and DEM raster are analyzed by comparing profile graphs of randomly selected locations. This profile graph comparison is conducted to visualize the vertical precision of the DEM raster and the TIN.

4.1.1 Dean Keaton Profile Graphs

The first location selected randomly is at Dean Keaton Street after the intersection with Speedway Street going from west to east. Figure 4.1 shows a zoom-in to this location, which is selected to analyze the cross section and longitudinal profile graphs of a TIN and DEM raster of a street.

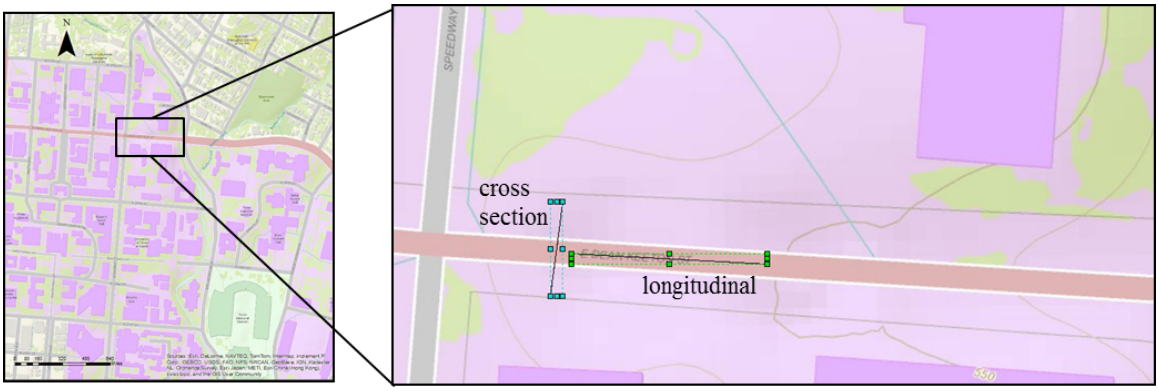

Figure 4.1: Location randomly selected at Dean Keaton Street for analyzing the cross section and longitudinal profile graphs of the Tin and DEM raster

Figure 4.2 shows the cross section profile graphs of the TIN and DEM raster generated with Airborne LiDAR data of the location at Dean Keaton Street. These profiles graphs are generated with the 3-D Analyst toolbar in ArcMap.

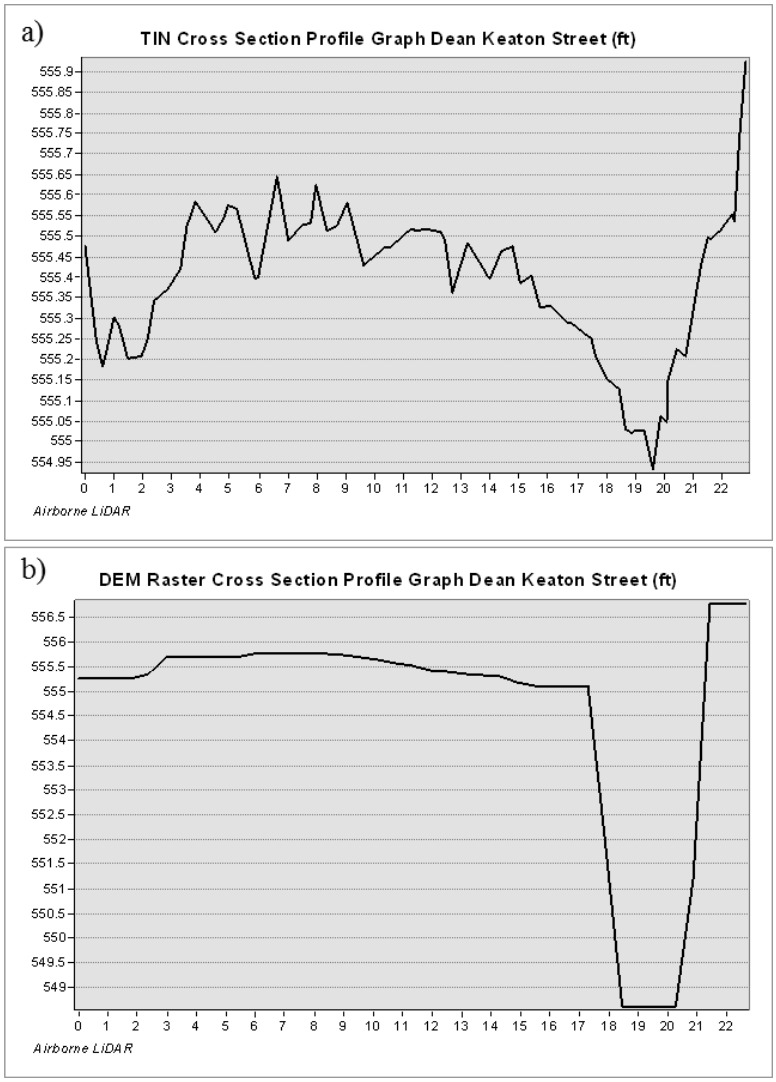

Figure 4.2: Cross section profile graphs of the a) TIN and b) DEM raster generated with Airborne LiDAR data of location at Dean Keaton Street

The DEM raster takes the average elevation of the points comprised in each cell, which gives more clear cross sections but is less precise than the TIN's elevation data at each point.

In October 2013 Mandli Communications collected Ground-based LiDAR data of UT's main campus area. This data has not been classified entirely, but a preliminary TIN

was generated for the area of Dean Keaton Street after the intersection with Speedway Street going from west to east. Figure 4.3 shows the cross section profile graph of the TIN generated with unclassified Ground-based LiDAR data. The cross section illustrated in Figure 4.3 is more clear and precise than the ones generated with Airborne LiDAR data. The TIN generated with Ground-based LiDAR data takes into consideration more elevation points than the TIN from Airborne LiDAR, which allows obtaining more clear cross sections and precise elevation data at each point.

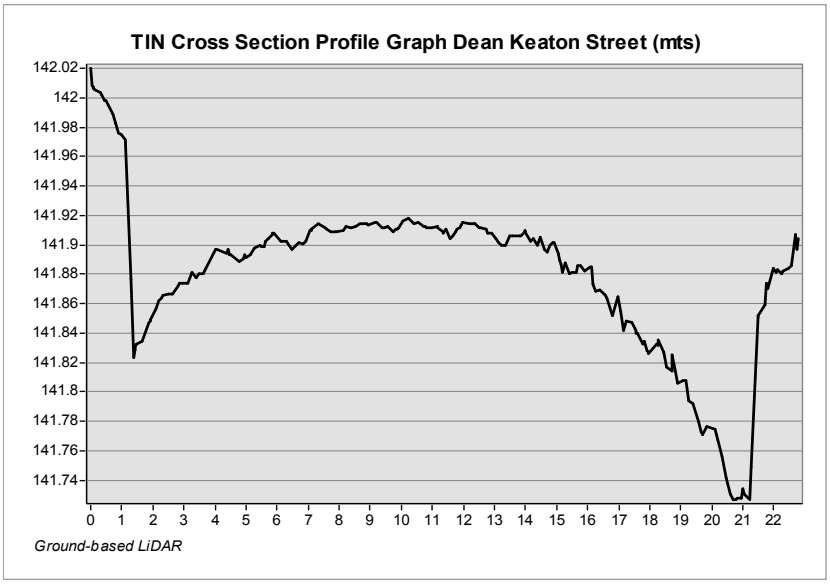

Figure 4.3: Cross section profile graph of the TIN generated with Ground-based LiDAR data of location at Dean Keaton Street

Figure 4.4 shows the longitudinal profile graphs of the TIN and DEM raster generated with Airborne LiDAR. These profiles graphs are generated with the 3-D Analyst toolbar in ArcMap.

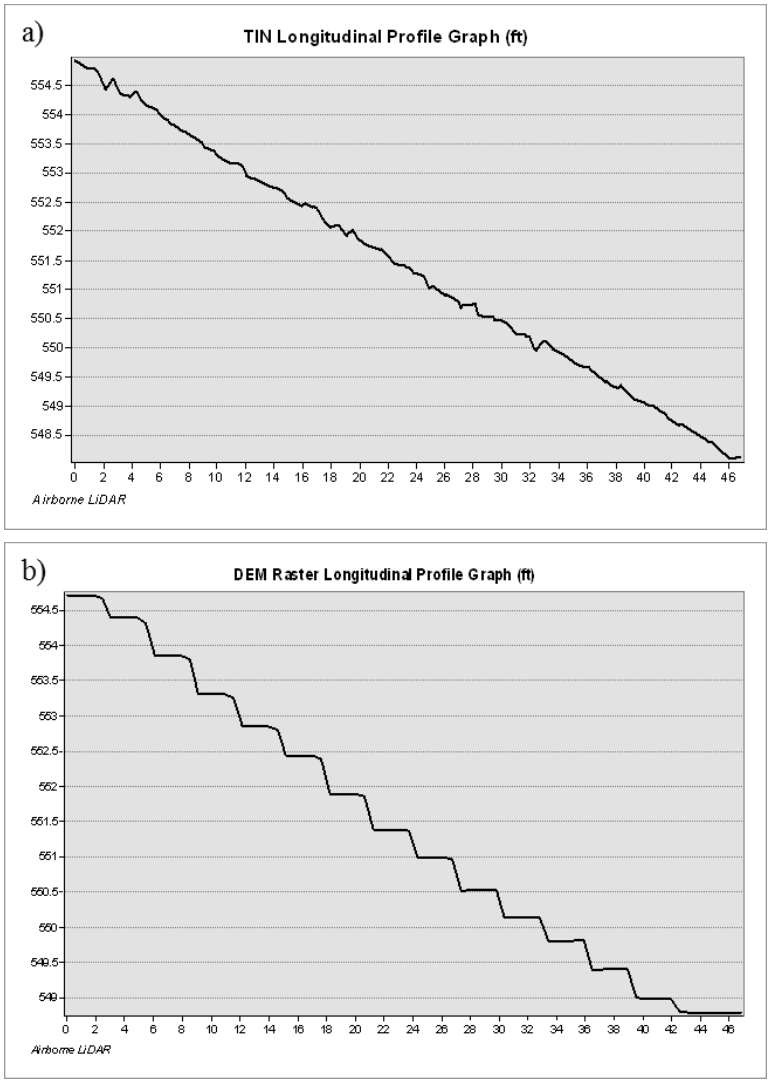

Figure 4.4: Longitudinal profile graphs of the a) TIN and b) DEM raster generated with Airborne LiDAR data of location at Dean Keaton Street

As Figure 4.4 illustrates, the TIN's longitudinal profile graph is more precise than the DEM Raster. The profile graph of the DEM raster file displays the profile as a ladder, which exemplifies the cell structure of a raster file and therefore suggests a lost in accuracy by using the DEM raster file rather than the TIN.

Figure 4.5 illustrates the longitudinal profile graph of the TIN generated with Ground-based LiDAR. This profile graph is generated with the 3-D Analyst toolbar in ArcMap. As Figure 4.5 shows, the TIN generated using Ground-based LiDAR has the highest definition of the longitudinal profiles of Dean Keaton Street after the intersection with Speedway Street going from west to east, which suggests that the Ground-based LiDAR files presents the more accurate elevation values of streets.

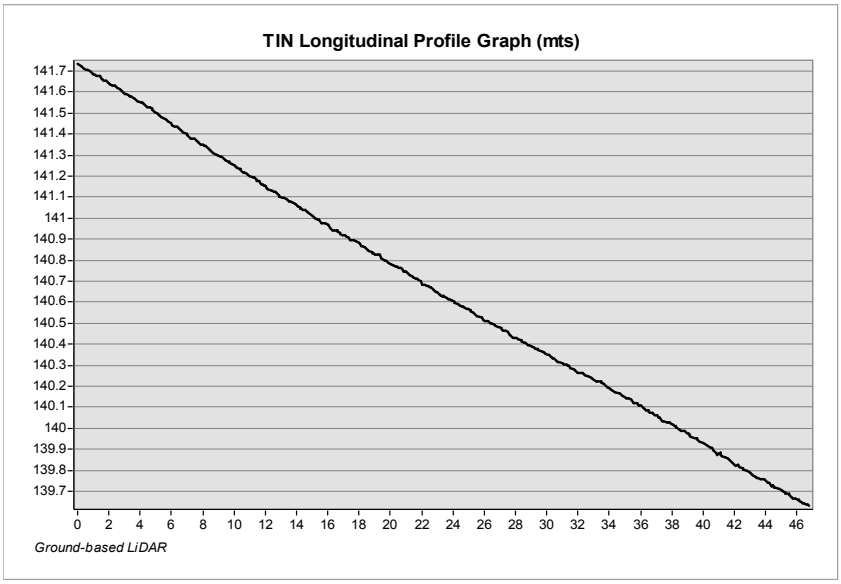

Figure 4.5: Longitudinal profile graph of the TIN generated with Ground-based LiDAR data of location at Dean Keaton Street

4.1.2 Texas Memorial Stadium Profile Graphs

The second location selected randomly for analyzing the TIN and DEM raster results is at UT's Memorial Stadium (Figure 4.6).

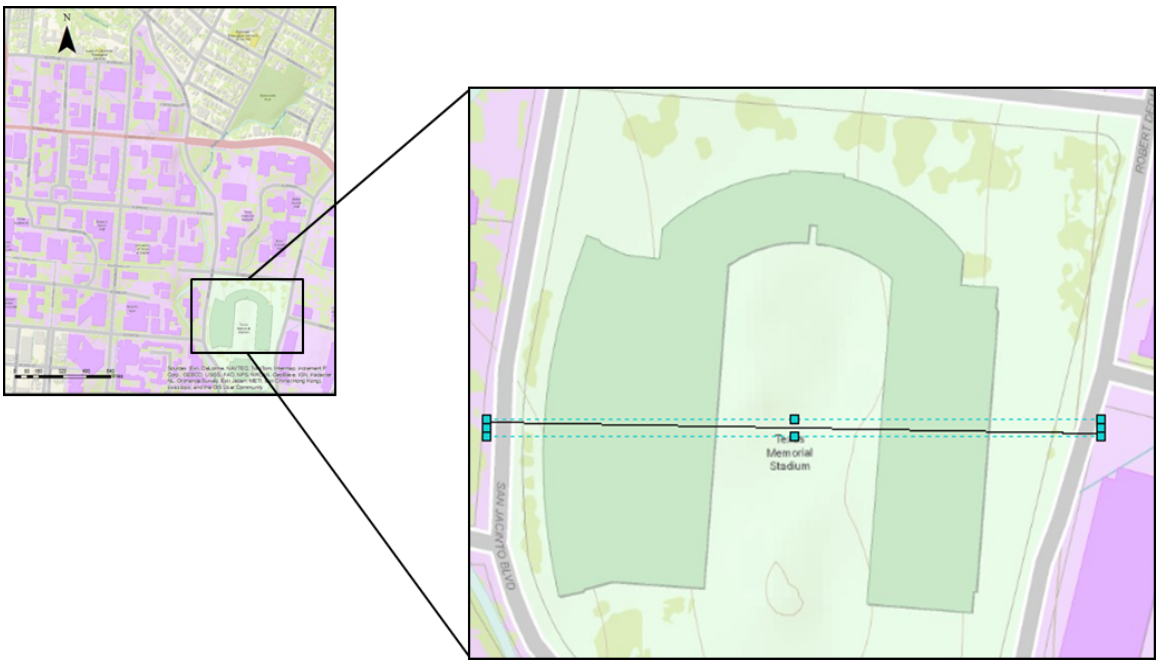

Figure 4.6: Location randomly selected at UT's Memorial Stadium for analyzing the profile graphs of the TIN and DEM raster

Figure 4.7 shows the profile graphs of the TIN and DEM raster generated with Airborne LiDAR elevation data of the selected location at UT's Memorial Stadium. These profiles graphs are generated with the 3-D Analyst toolbar in ArcMap. As Figure 4.7 shows, the profile graph from the TIN delineates better the cross section of UT's Memorial Stadium than the DEM raster. Furthermore, the profile graph of the DEM raster displays the cells of the raster as steps, which exemplifies the loose of accuracy by transforming the TIN to a DEM raster.

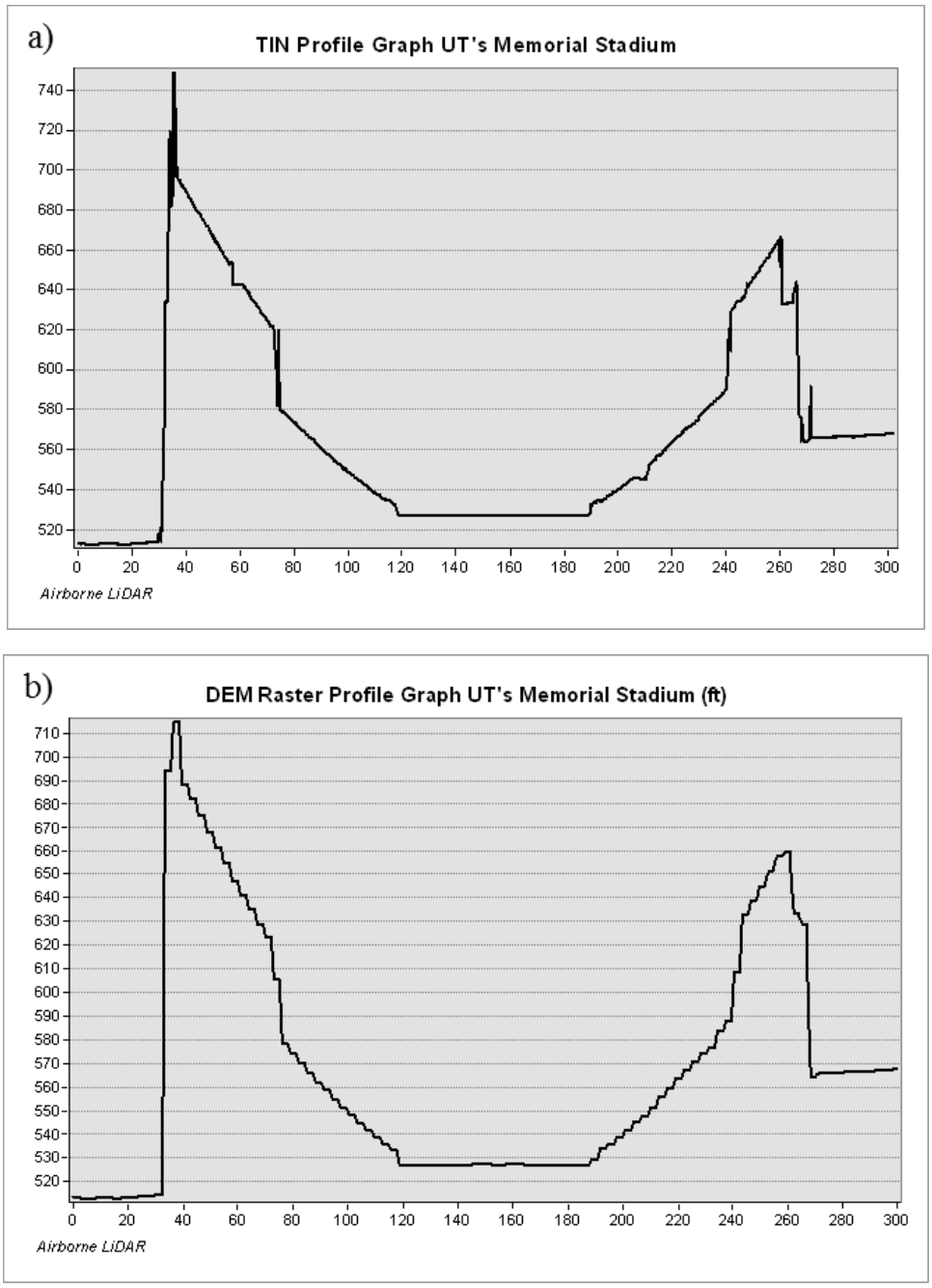

Figure 4.7: Profile graphs of the a) TIN and b) DEM raster generated with Airborne LiDAR data of a selected location at UT's Memorial Stadium

4.1.2 UT's Main Building Profile Graphs

As Figure 4.8 shows, the third location selected randomly for comparing the TIN and DEM raster profile graphs is at UT's Main Building.

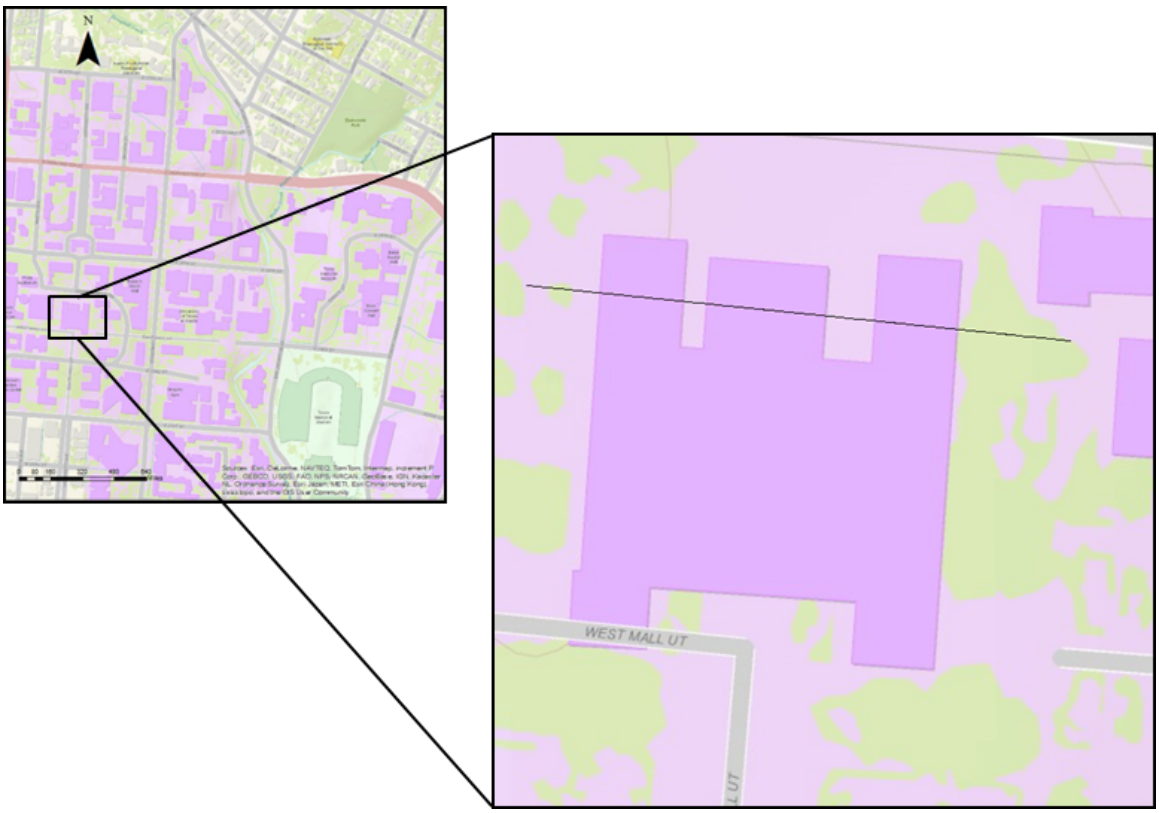

Figure 4.8: Location randomly selected at UT's Main Building for analyzing the profile graphs of the Tin and DEM raster

Figure 4.9 shows the profile graphs of the TIN and DEM raster generated with Airborne LiDAR elevation data of the selected location at UT's Main Building. These profiles graphs are generated with the 3-D Analyst toolbar in ArcMap. As Figure 4.9 shows, the profile graph from the TIN outlines the cross section of UT's Main building more precisely than the DEM raster. Moreover, the profile graph of the DEM raster

displays a cut in the higher point of the tower of the main building, which suggests loose of accuracy due to the interpolation of the elevation points at the raster's cells.

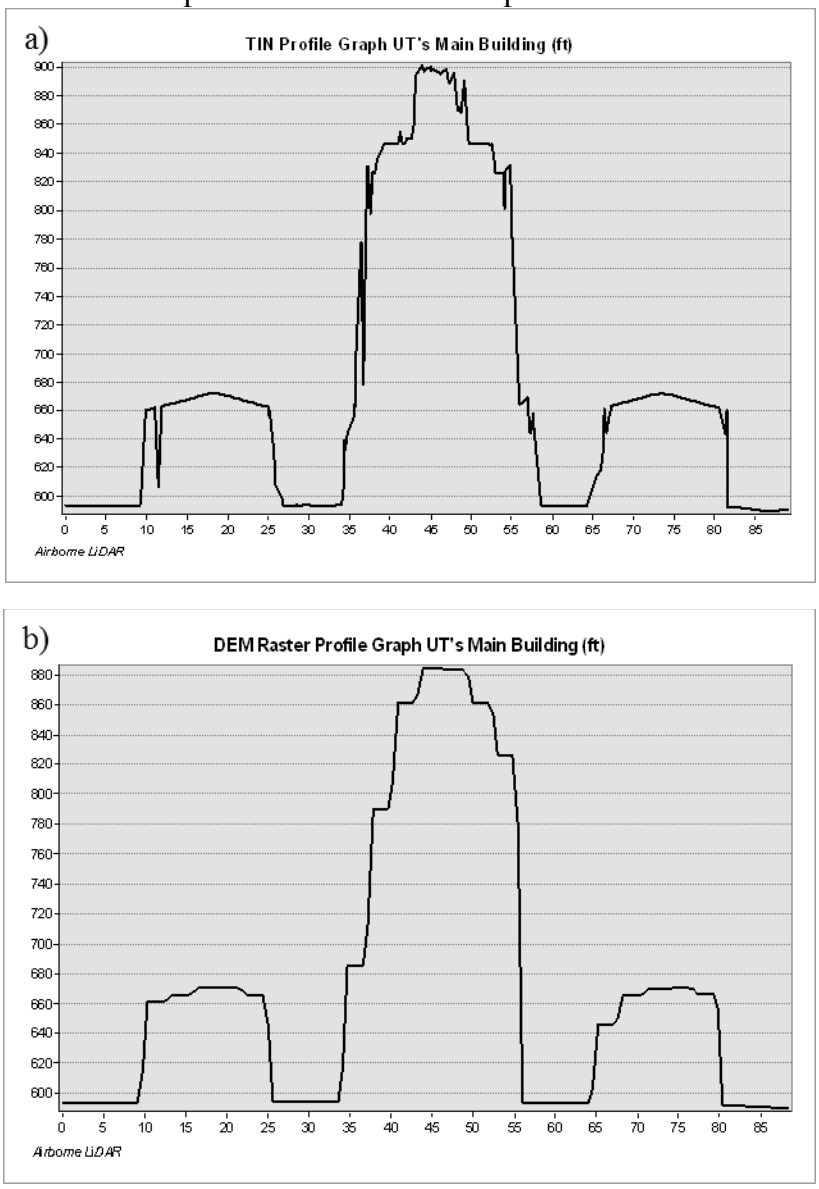

Figure 4.9: Profile graphs of the a) TIN and b) DEM raster generated with Airborne LiDAR data of a selected location at UT's Main Building

4.2 MODELING STORMWATER SEWER SYSTEM WITH HIGH RESOLUTION DATA

The stormwater sewer system of the northwest area of the main campus of UT can be divided as following:

1. *Stormwater Sewer System 1*. This is the stormwater sewer system that discharges to Waller Creek from the parking lot of the Animal Resources Center (Figure 4.10).

   The results obtained from modeling this stormwater sewer system are analyzed for 4 scenarios (2, 10, 25 and 100 years) with 1) the profile graphs of the system that shows its energy and hydraulic gradient levels, and 2) the ratio of flow to the total capacity of the pipelines. Figure 4.11 and Figure 4.12 presents the profile graphs of the Stormwater Sewer System 1 that shows the energy and hydraulic gradient levels of the principal pipelines of this system. As Figure 4.11 and Figure 4.12 shows, the hydraulic response of this system is affected by the water surface elevation at the discharge point to Waller Creek, where the tailwater level is higher than the outfall pipe crown. This water surface elevation causes the system to flow almost to its full capacity for a 100-year event; however, Figure 4.11 and Figure 4.12 suggests that the Stormwater Sewer System 1 is adequate for the scenarios modeled.

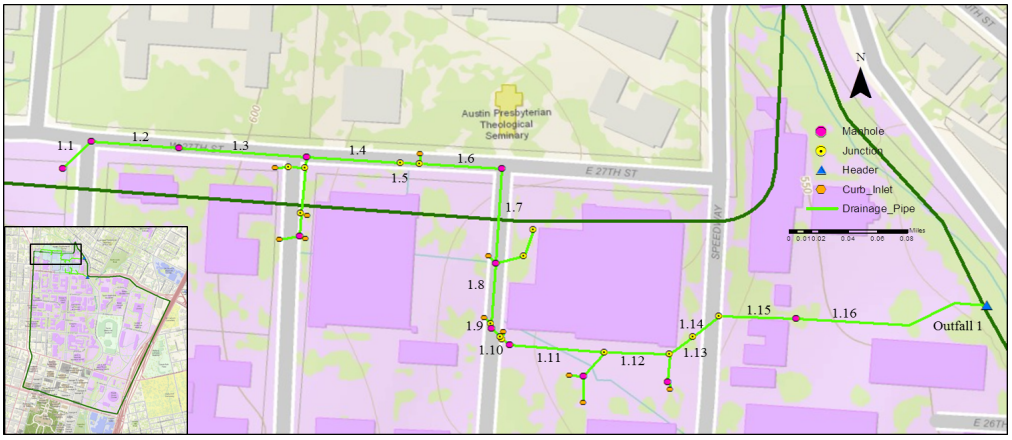

Figure 4.10: The stormwater sewer system that discharges to Waller Creek from the parking lot of the Animal Resources Center

Figure 4.11: Profile graphs showing the energy and hydraulic gradient levels of the principal pipelines of the Stormwater Sewer System 1 for an a) 2-yr, and b) 10-yr

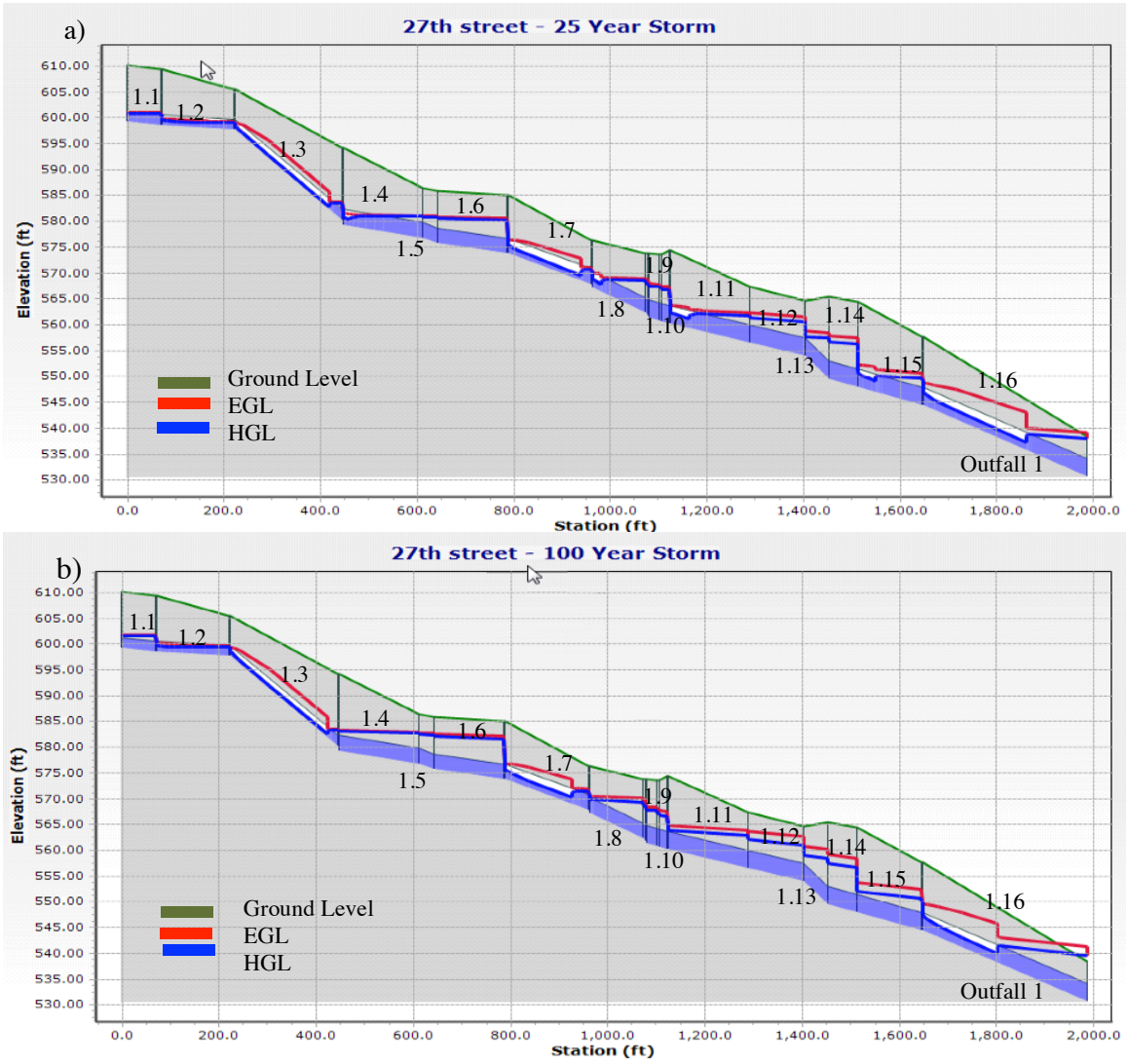

Figure 4.12: Profile graphs showing the energy and hydraulic gradient levels of the principal pipelines of the Stormwater Sewer System 1 for an a) 25-yr, and b) 100-yr storm event

Table 4.1 presents the performance of the pipelines as a percentage of the total capacity occupied by the flow in each scenario. As Table 4.1 shows, the maximum percentage of this ratio for all scenarios is lower than 100% at all times, which suggests that the drainage system is adequate for preventing flooding in the area of the Stormwater Sewer System 1.

Table 4.1: The ratio of the flow to the total capacity of the pipelines in the sewer system that discharges to Waller Creek from the parking lot of the Animal Resources Center

Pipeline Label	Ratio of Flow to the Total Capacity (%)			
	2 year	10 year	25 year	100 year
1.1	15.60%	26.20%	32.80%	45.50%
1.2	20.30%	34%	42.70%	58.90%
1.3	5.50%	9.30%	11.60%	16.10%
1.4	16.50%	24.80%	29.80%	38.60%
1.5	25.20%	36.90%	43.70%	54.80%
1.6	15.40%	22.10%	26.40%	33.30%
1.7	14.70%	21.50%	25.90%	33%
1.8	18.30%	25.60%	30.20%	37.70%
1.9	14.50%	20.30%	24%	29.90%
1.10	24.90%	35.20%	41.70%	51.80%
1.11	24.80%	35.10%	41.50%	51.70%
1.12	29.50%	42.90%	51.50%	65%
1.13	15.80%	23%	27.70%	35.10%
1.14	29%	42.20%	50.70%	64.40%
1.15	27.70%	40.50%	48.70%	61.90%
1.16	22.40%	32.80%	39.50%	50.10%
1.17	20.40%	29.40%	34%	42.90%
1.18	3%	5%	6.30%	8.60%
1.19	2.90%	4.90%	6.20%	8.40%
1.20	20.30%	28.50%	33%	40.60%
1.21	0.40%	0.60%	0.80%	1.20%
1.22	16.10%	22.40%	25.80%	31.40%
1.23	8.40%	11.30%	12.70%	15%
1.24	2.20%	3.60%	4.50%	6%
1.25	11.10%	16.80%	20.20%	25.80%
1.26	5.30%	7.20%	8.20%	9.80%
1.27	2.80%	4.70%	5.80%	8%
1.28	10.60%	18%	22.60%	31.60%
1.29	2.80%	4.70%	5.90%	8.20%
1.30	8.40%	10.80%	12.10%	14.10%
1.31	8.10%	12.20%	14.30%	17.50%
1.32	8.20%	13.90%	17.30%	22.80%
1.33	5.80%	9.70%	12%	15.50%
1.34	2.10%	3.60%	4.60%	6.50%
1.35	7.30%	12.20%	15%	19.80%
1.36	11.10%	18.40%	22.60%	29.70%
1.37	18.40%	25.80%	30.50%	38%

2. *Stormwater System 2*. This is the stormwater system that discharges to Waller Creek from Dean Keaton Street (Figure 4.13). Following the analysis of the Stormwater Sewer System 1, the results obtained from modeling the Stormwater Sewer System 2 are interpreted for 4 scenarios (2, 10, 25 and 100 years) with 1) the ratio of flow to the total capacity of the pipelines, and 2) the profile graphs of the system that illustrates its energy and hydraulic gradient levels. Figure 4.14 and Figure 4.15 illustrates the profile graphs of the Stormwater Sewer System 2, which shows the energy and hydraulic gradient levels of the principal pipelines of the system. As Figure 4.14 and Figure 4.15 presents, the hydraulic response of the system is affected by the water surface elevation at the discharge point to Waller Creek, where the tailwater level is higher than the outfall pipe crown. This hydraulic response can be observed by analyzing the increase in the gradient levels for each scenario. Furthermore, the manhole at the intersection of Dean Keaton and the engineering footbridge (circle in orange in Figure 4.15) appears to be soaked for a 25 and 100 year storm event. In other words, Figure 4.15 suggests that the drainage system is not adequate for preventing flooding in the area of the Stormwater Sewer System 2 for a 25 and 100 year storm events.

Figure 4.13: The stormwater system that discharges to Waller Creek from Dean Keaton Street

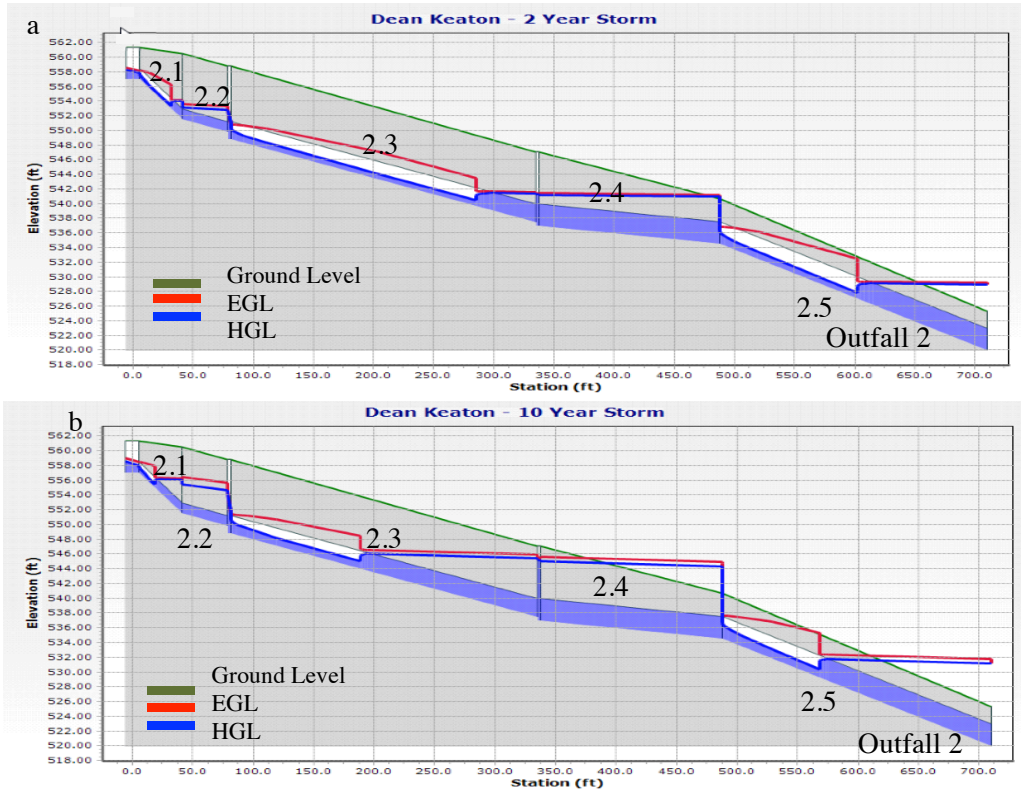

Figure 4.14: Profile graphs showing the energy and hydraulic gradient levels of the principal pipelines of the Stormwater Sewer System 2 for an a) 2-yr, and b) 10-yr

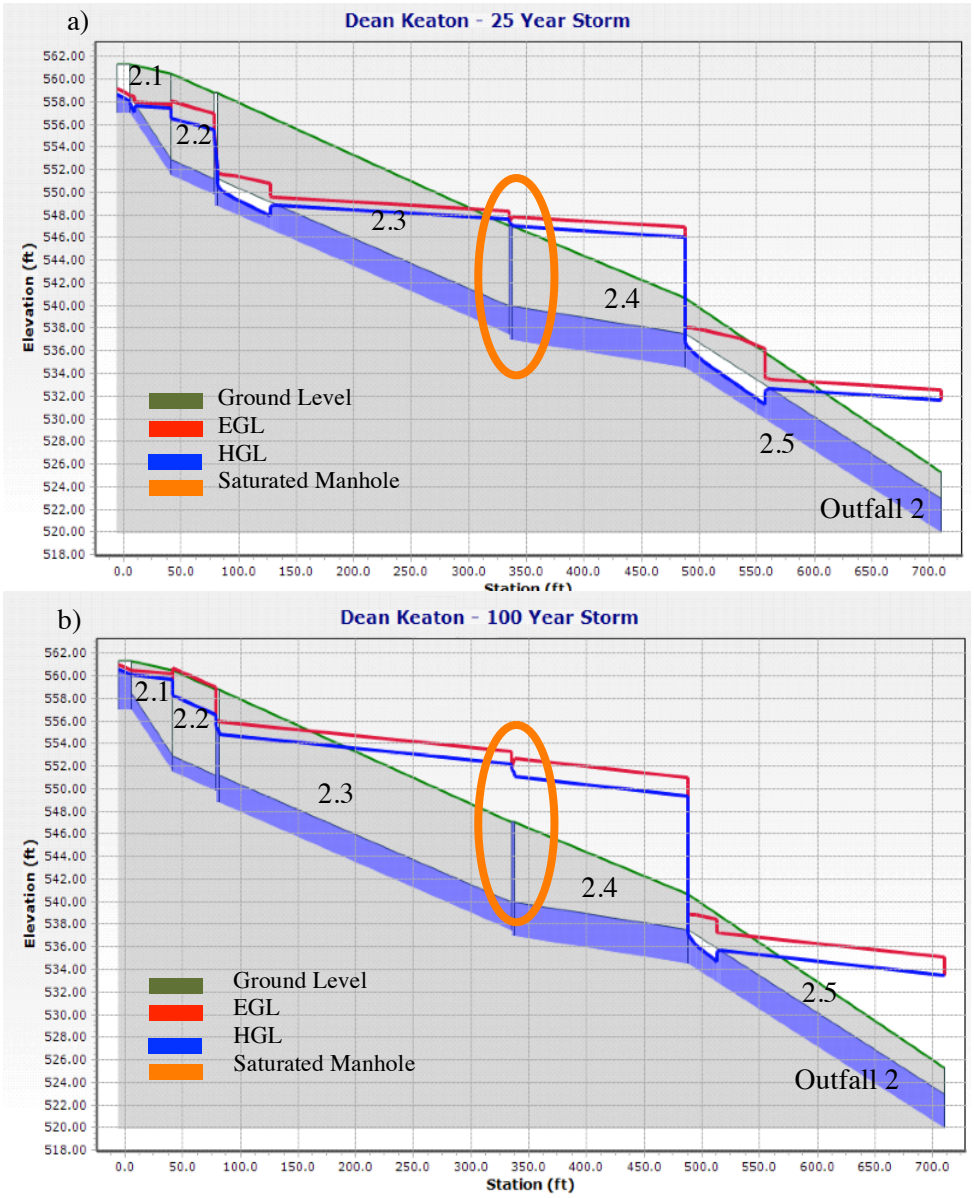

Figure 4.15: Profile graphs showing the energy and hydraulic gradient levels of the principal pipelines of the Stormwater Sewer System 2 for an a) 25-yr, and b) 100-yr storm event

Table 4.2 shows the performance of the pipelines as a percentage of the total capacity occupied by the flow in each scenario. As Table 4.2 presents, the

pipeline with unique label 2.2 (Figure 4.16) has a percentage higher than 100% for the 100-year event scenario, which reasserts that the drainage system is not adequate for preventing flooding in the area of the Stormwater Sewer System 2. Figure 4.16 shows the pipeline with unique label 2.2, which is located at the intersection of Dean Keaton Street and Speedway.

Table 4.2: The ratio of the flow to the total capacity of the pipelines in the sewer system that discharges to Waller Creek from Dean Keaton Street

Pipeline Label	Ratio of Flow to the Total Capacity			
	2-yr	10-yr	25-yr	100-yr
2.1	12.60%	17.80%	20.40%	24.40%
2.2	42.50%	65.60%	77.30%	100.80%
2.3	21.10%	32.40%	37.80%	48.40%
2.4	32.70%	52.90%	63.50%	83.70%
2.5	15.80%	25.80%	31.10%	41.20%
2.6	26.20%	36.40%	41.50%	49.50%
2.7	9.40%	16.20%	19.70%	25%
2.8	29.70%	45.30%	53.20%	65.20%
2.9	12.90%	21.60%	27.10%	37.40%
2.10	19%	31.80%	39.90%	55.30%
2.11	4.30%	7%	8.80%	11.40%
2.12	5.10%	8.50%	10.60%	13.70%
2.13	17.80%	29.40%	36.80%	50.50%
2.14	13.10%	23.10%	29.20%	39.60%
2.15	1%	1.70%	2.20%	3.30%

Figure 4.16: Pipeline with unique label 2.2 has a ratio of flow to the total capacity higher than 100% for a 100-yr scenario.

4.3 Modifying Stormwater Sewer Systems Using the HydroDesign Framework

The stormwater sewer system that discharges to Waller Creek from Dean Keaton Street can be under strain for 25 and 100 year storm events. Figure 4.15 and Table 4.2 suggests that the main drivers of the inefficiency of the system are 1) the water surface level of Waller Creek at the discharge, and 2) the size of the pipeline at the intersection of Dean Keaton Street and Speedway Street. In order to improve the capacity and response of this stormwater sewer system, an application of the framework of GeoDesign to stormwater systems is used to obtain a feasible solution. The application of this framework to stormwater systems is illustrated in Figure 4.17.

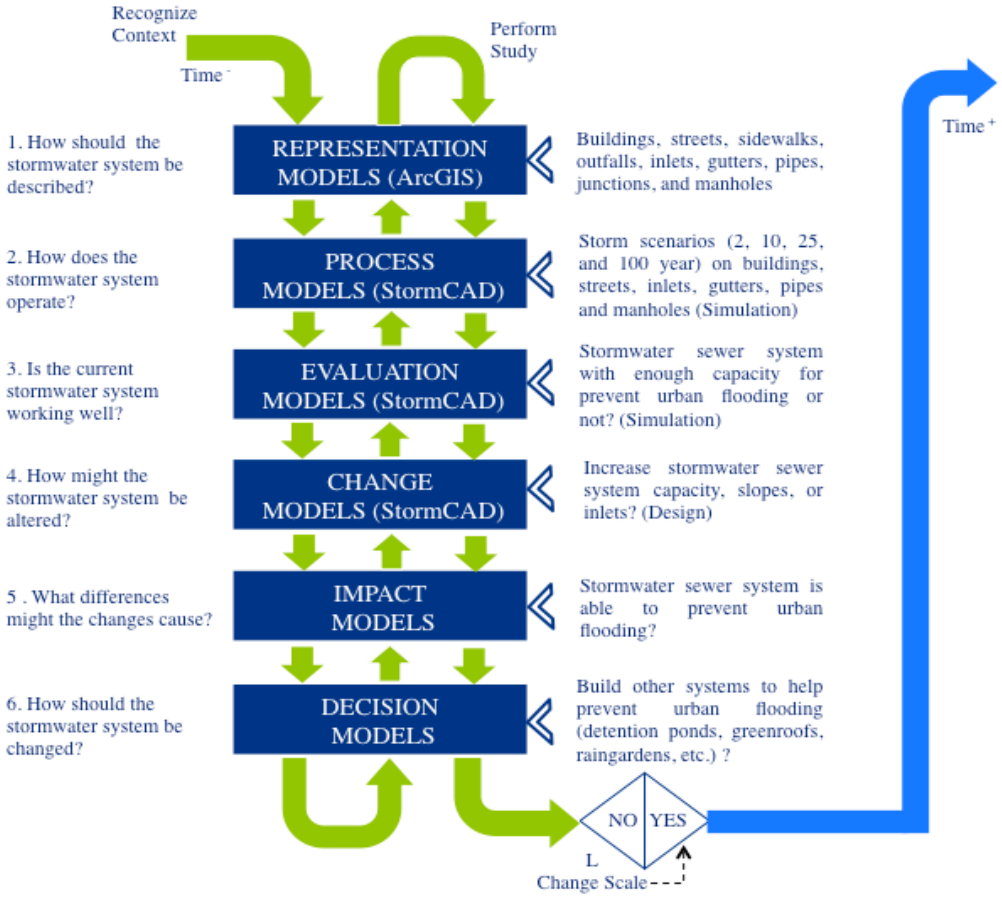

Figure 4.17: Diagram adapted from Steinitz (2012) GeoDesign framework applied to stormwater sewer systems.

According to Figure 4.15, if the system does not have enough capacity (Evaluation Models) an increase in the sizes of the pipes has to be made (Change Models). The increase suggested in this stormwater sewer system is in 1) the last two pipes of the system from 36 to 48 inches, and 2) the pipe of the intersection of Speedway and Dean Keaton Street from 18 to 30 inches. Figure 4.18 presents the profile graphs of the modified stormwater sewer system for the 25 and 100 year storm scenarios, which shows the energy and hydraulic gradient levels of the principal pipelines of this system. As Figure 4.18 illustrates, the hydraulic response of the modified system is still affected

by the water surface elevation at the discharge point to Waller Creek, where the tailwater level is higher than the outfall pipe crown. However, the modified system is no strained over capacity. Additionally, the manhole that appeared to be soaked for 25 and 100 year storm events in the system's current condition (Figure 4.15) is no longer saturated for the modified system (Figure 4.18).

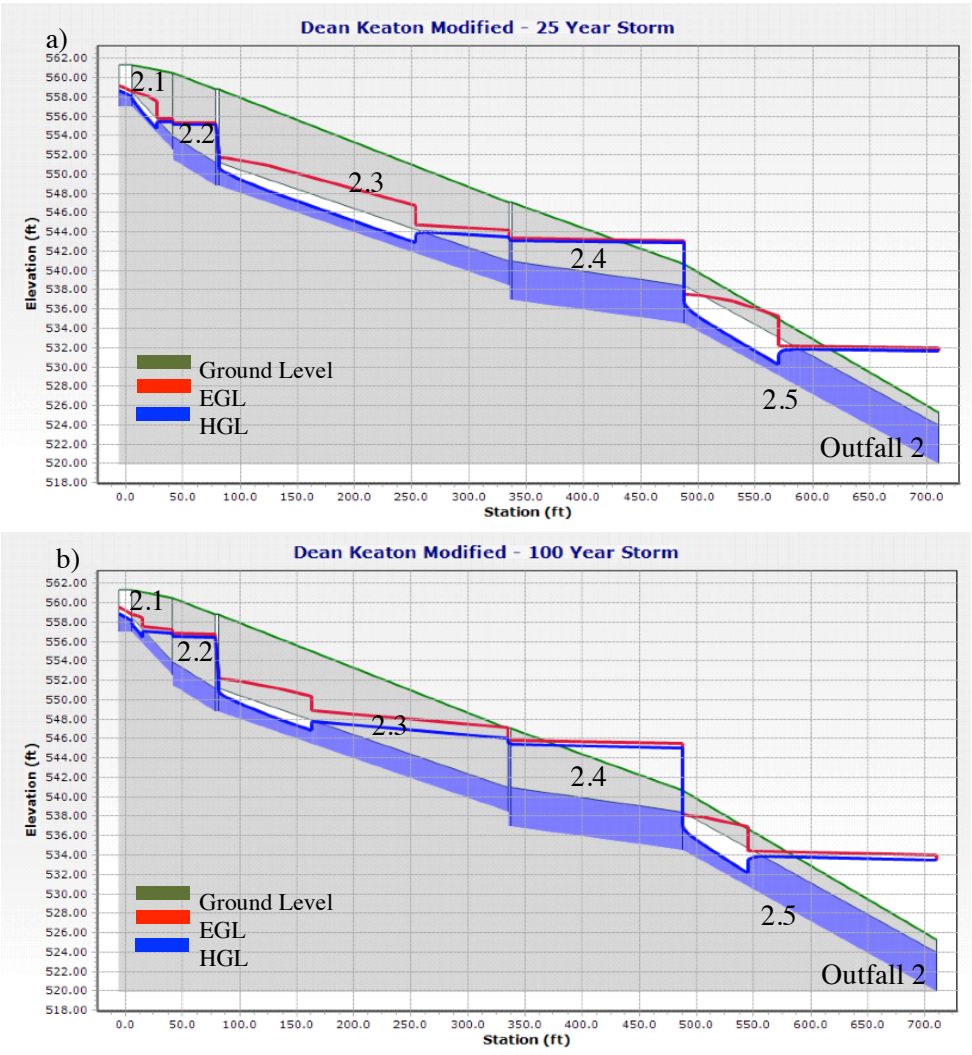

Figure 4.18: Profile graphs showing the energy and hydraulic gradient level of the principal pipelines of the modified Stormwater Sewer System 2 for a storm event with return period of a) 25-yr, and b) 100-yr

Furthermore, Table 4.3 presents the percentage of the total capacity occupied by the flow in each scenario for the modified sewer system that discharges to Waller Creek from Dean Keaton Street. As Table 4.3 shows, the maximum percentage of this ratio for all scenarios is lower than 100% at all times, which suggests that the drainage system is adequate for preventing flooding in the area of the modified system.

Table 4.3: The ratio of the flow to the total capacity of the pipelines of the modified system that discharges to Waller Creek from Dean Keaton Street

Pipeline Label	Ratio of Flow to the Total Capacity (%)			
	2 year	10 year	25 year	100 year
2.1	14.0%	19.7%	22.6%	27.0%
2.2	8.6%	13.4%	16.1%	20.5%
2.3	22.1%	33.8%	40.4%	50.6%
2.4	15.2%	24.5%	30.0%	39.1%
2.5	7.5%	11.8%	14.5%	19.1%
2.6	26.2%	36.4%	41.5%	49.5%
2.7	9.4%	16.2%	19.7%	25.0%
2.8	29.7%	45.3%	53.2%	65.2%
2.9	12.9%	21.6%	27.1%	37.4%
2.10	19.0%	31.8%	39.9%	55.3%
2.11	4.8%	8.0%	9.9%	12.9%
2.12	5.1%	8.5%	10.6%	13.7%
2.13	17.8%	29.4%	36.8%	50.5%
2.14	14.6%	25.8%	32.5%	44.2%
2.15	1.1%	1.9%	2.4%	3.7%

Chapter 5: Conclusions

5.1 Stormwater Sewer Systems Evaluation Methodology

Stormwater sewer systems are built to remove stormwater from the site as quickly and efficiently as possible. Urban floods can be caused by inefficient stormwater sewer systems, which need to be evaluated for different storm event scenarios. The procedure developed integrated high-resolution data, ArcGIS, and StormCAD to evaluate current storm water infrastructure. This evaluation is crucial in the decision making process of urban planning to prevent and mitigate floods in urban areas.

Current methodologies use low-resolution DEM raster files and/or topographic maps from field measurements to obtain the stormwater systems elements' characteristics. The vertical accuracy of a low-resolution DEM raster fluctuates between 2 and 15m (Ritchie, 2009), while field measurements are time consuming and do not give a continuous representation of elevation points in space. On the other hand, the methodology employed in the present work used high-resolution data obtained from an Airborne LiDAR system. Airborne LiDAR systems usually have a point spacing distance between 30 and 60 cm, and a vertical accuracy around 15 cm (Lim et al., 2003).

The high-resolution elevation data from the Airborne LiDAR system enabled us to estimate the ground elevation, identify ground obstructions, detect water flowpaths, and digitize the drainage areas more precisely. Nonetheless, as Figure 4.3 and Figure 4.5 suggest, the use of Ground-based LiDAR would allow obtaining even more precise data of streets and sidewalks. Ground-based LiDAR systems collect around 1 million points per second (Mandli Communications 2013), which translates in obtaining higher-resolution data to digitize streets, parking lots, sidewalks, and bridges.

The processing of Airborne LiDAR data, digitization, and characterization of the stormwater drainage system is computed in ArcMap, which is part of ArcGIS' suite of GIS geospatial processing software. Traditional methodologies use specialized software such as StormCAD, SWMM, or Hydra for modeling and evaluating stormwater sewer systems. The methodology presented in this thesis employs StormCAD, which allowed evaluating different storm events alternatives for each scenario analyzed. The steps StormCAD follows to run the model are 1) generate surface loads and perform inlets' computation, 2) route intercepted loads downstream through the pipelines, and 3) compute headlosses upstream through the pipelines (StormCAD Users Guide 2013).

As Table 4.1 shows, the capacity of the system that discharge to Waller Creek from the parking lot of the Animal Resources Center is able to prevent floods for 2, 10, 25, and 100 year storm events. On the other hand, Table 4.2 suggests that the sewer system that discharges to Waller Creek from Dean Keaton Street does not have the capacity for 25 and 100 year storm events.

5.2 Future Work and Research

The digitization of UT's stormwater sewer system can be integrated to a greater project called The Digital Campus of The University of Texas at Austin. The Digital Campus is a compilation of data that intends to describe the 3-D layout and environmental conditions of UT's main campus. Further work and research is required to construct a truthful 3-D model of UT's main campus, which has to incorporate current infrastructure that will assist in the design process of future planning in the campus. The Digital Campus can incorporate the concept of GeoDesign, which is defined by Steinitz (2012) as "the development and application of design related procedures intended to change the geographical study areas in which they are applied and realized".

Furthermore, Dr. David Maidment has defined HydroDesign, which follows the framework of GeoDesign, in order to evaluate and plan the way people interact with water in their surroundings.

The principal concern of HydroDesign is to assist in the design process to mitigate flood impacts, use water efficiently, and prevent water pollution. Therefore, future work and research has to be conducted to integrate and evaluate 1) UT's complete stormwater sewer system, 2) UT's water distribution system, and 3) UT's sewer drainage system. Moreover, a procedure to integrate Airborne and Ground-based LiDAR in one TIN has to be developed to describe with the highest-resolution available the elements that comprise The Digital Campus. In other words, research has to be conducted to select 1) the buildings' multipoints from the Airborne LiDAR data, and 2) the terrain's multipoints from Ground-based LiDAR. The most important limitation for integrating the Airborne and Ground-based LiDAR files lies on the difficult and time consuming task of classifying the points from Ground-based LiDAR. For this limitation, new tools have to be developed to achieve a faster and precise classification of LiDAR data files. Integrating the Airborne and Ground-based LiDAR data files will represent a great progress in order to achieve truthful 3-D models of the main campus of UT.

Additionally, it is essential to indicate that the period of record used for generating the different scenarios of the present work are based on the Drainage Criteria Manual (2013) of The City of Austin; however, further research has to be conducted integrating the factor of climate change that could affect the values obtained. In other words, the hydrology in the catchment is not stationary due to climate change, which can provoke changes in 1) upstream conditions; and 2) precipitation patterns, intensities, and frequencies.

References

Abdullah, a. F., Vojinovic, Z., Price, R. K., & Aziz, N. a. a. (2012). A methodology for processing raw LiDAR data to support urban flood modeling framework. *Journal of Hydroinformatics*, *14*(1), 75. doi:10.2166/hydro.2011.089

American Society and Photogrammetry and Remote Sensing. (2013). *LAS SPECIFICATION Version 1.4-R13* (pp. 1–28).

Andersen, H., Reutebuch, S. E., & Mcgaughey, R. J. (2006). ACTIVE REMOTE SENSING. In G. Shao & K. M. Reynolds (Eds.), Computer Applications in Sustainable Forest Management Including Perspectives on Collaboration and Integration (pp. 43–66). Springer.

ArcGIS Resources. (2013). Types of LiDAR. ArcGIS Help 10.1. Retrieved from http://resources.arcgis.com/en/help/main/10.1/index.html#//015w00000052000000

British Geological Service. (2013). BGS subsurface information relevant to SuDS and infiltration. Retrieved from http://www.bgs.ac.uk/science/landUseAndDevelopment/urban_geoscience/SUDS/information.html

Champagne, J.-Y., Haider, S., Paquier, a., & Morel, R. (2003). Urban flood modeling using computational fluid dynamics. *Proceedings of the ICE - Water and Maritime Engineering*, *156*(2), 129–135. doi:10.1680/wame.2003.156.2.129

Chen, A. S., Evans, B., Djordjević, S., & Savić, D. a. (2012). Multi-layered coarse grid modeling in 2D urban flood simulations. *Journal of Hydrology*, *470-471*, 1–11. doi:10.1016/j.jhydrol.2012.06.022

Chow, V. Te, Maidment, D. R., & Mays, L. W. (1988). *Applied Hydrology*. (B. J. Clark & J. Morriss, Eds.) (Internatio.). McGraw-Hill.

Chu, M. L., Knouft, J. H., Ghulam, a., Guzman, J. a., & Pan, Z. (2013). Impacts of urbanization on river flow frequency: A controlled experimental modeling-based evaluation approach. *Journal of Hydrology*, *495*, 1–12. doi:10.1016/j.jhydrol.2013.04.051

City of Austin, T. (2013). *Drainage Criteria Manual*. American Legal Publishing Corporation.

Crossley, M., Lamb, R., & Waller, S. (2009). A fast two-dimensional floodplain inundation model. *Proceedings of the ICE - Water Management*, *162*(6), 363–370. doi:10.1680/wama.2009.162.6.363

Curran, P. J. (2014). Geographic information systems, *16*(2), 153–158.

Dangermond, J. (2009). GIS: Designing Our Future. *ArcNews Online*. Retrieved from http://www.esri.com/news/arcnews/summer09articles/gis-designing-our-future.html

Davis, A. P., & McCuen, R. H. (2005). *Stormwater Management for Smart Growth* (ebook.). Springer. Retrieved from <http://UTXA.eblib.com/patron/FullRecord.aspx?p=302849>.

Dingman, L. S. (2002). *Physical Hydrology* (Second Edi., pp. 1–89). Waveland Press, Inc.

Dottori, F., & Todini, E. (2013). Testing a simple 2D hydraulic model in an urban flood experiment. *Hydrological Processes*, *27*(9), 1301–1320. doi:10.1002/hyp.9370

Environmental Protection Agency. (2003). Urban Nonpoint Source Fact Sheet. Retrieved from http://water.epa.gov/polwaste/nps/urban_facts.cfm

Forsee, W. J., & Ahmad, S. (2011). Evaluating Urban Storm-Water Infrastructure Design in Response to Projected Climate Change, (November), 865–873. doi:10.1061/(ASCE)HE.1943-5584.0000383.

Jaboyedoff, M., Oppikofer, T., Abellán, A., Derron, M.-H., Loye, A., Metzger, R., & Pedrazzini, A. (2010). Use of LIDAR in landslide investigations: a review. *Natural Hazards*, *61*(1), 5–28. doi:10.1007/s11069-010-9634-2

Klipp, E., & Nayegandhi, A. (2007). USGS Hosts Airborne-Lidar Technology and Applications Workshop in Louisiana. *United States Geological Survey*.

Leitão, J. P., Simões, N. E., Maksimović, C., Ferreira, F., Prodanović, D., Matos, J. S., & Sá Marques, a. (2010). Real-time forecasting urban drainage models: full or simplified networks? *Water Science and Technology : A Journal of the International Association on Water Pollution Research*, *62*(9), 2106–14. doi:10.2166/wst.2010.382

Li, Z., Zhu, Q., & Gold, C. (2005). *Digital Terrain Modeling Principles and Methodology* (pp. 1–111). CRC Press.

Lim, K., Treitz, P., Wulder, M., St-Onge, B., & Flood, M. (2003). LiDAR remote sensing of forest structure. *Progress in Physical Geography*, *27*(1), 88–106. doi:10.1191/0309133303pp360ra

Liu, X. (2008). Airborne LiDAR for DEM generation: some critical issues. *Progress in Physical Geography*, *32*(1), 31–49. doi:10.1177/0309133308089496

Maidment, D. R. (2002). *Arc hydro: GIS for water resources*. ESRI Press. Retrieved from http://books.google.com/books?id=1WRvmYju-nkC

Maidment, D. R. (2013). HydroDesign and the Digital Campus. Retrieved from http://www.ce.utexas.edu/prof/maidment/CE365KSpr14/Docs/HydroDesign.pdf

Mandli Communications. (2013). No. Retrieved from http://www.mandli.com/applications/

Mays, L. W. (2001). *Stormwater Collection Systems Design Handbook*. McGraw-Hill. Retrieved from http://ezproxy.lib.utexas.edu/login?url=http://search.ebscohost.com/login.aspx?direct=true&db=nlebk&AN=63611&site=ehost-live

Meyer, B. S. P., Salem, T. H., Member, S., & Labadie, J. W. (1993). Storm-Water Management Integrated DSS Development The integrated development approach uses customized programs that, *119*(2), 206–228.

National Oceanic and Atmospheric Administration's. (2013). Hydrologic Information Center - Flood Loss Data. Retrieved from http://www.nws.noaa.gov/hic/

Novotny, V., Ahern, J., & Brown, P. (2010). Stormwater Pollution Abatement and Flood Control—Stormwater as a Resource. In *Water Centric Sustainable Communities* (pp. 177–227). Hoboken, NJ, USA: John Wiley & Sons, Inc. doi:10.1002/9780470949962.ch4

Pan, A., Hou, A., Tian, F., Ni, G., & Hu, H. (2012). Hydrologically Enhanced Distributed Urban Drainage Model and Its Application in Beijing City, (June), 667–678. doi:10.1061/(ASCE)HE.1943-5584.0000491.

Ritchie, J. C. (2009). Remote sensing applications to hydrology : airborne laser altimeters Remote sensing applications to hydrology : airborne laser altimeters, (January 2014), 37–41.

Schmid, K. A., Hadley, B. C., & Wijekoon, N. (2011). Vertical Accuracy and Use of Topographic LiDAR Data in Coastal Marshes. West Palm Beach (Florida): Journal of Coastal Research.

Seyoum, S. D., Vojinovic, Z., Price, R. K., Weesakul, S., & Ph, D. (2012). Coupled 1D and Noninertia 2D Flood Inundation Model for Simulation of Urban Flooding, (January), 23–34. doi:10.1061/(ASCE)HY.1943-7900

Smith, B. K., Smith, J. a., Baeck, M. L., Villarini, G., & Wright, D. B. (2013). Spectrum of storm event hydrologic response in urban watersheds. *Water Resources Research*, *49*(5), 2649–2663. doi:10.1002/wrcr.20223

Sole, A., Giosa, L., Nolè, L., Medina, V., Bateman, A., Università, D. I. F. A., & Catalunya, E. H. M. A. U. P. De. (n.d.). Flood risk modeling with LiDAR technology.

Steinitz, C. (2012). A Framework for Geodesign: Changing Geography by Design. ESRI Press.

Tsihrintzis, V. a., Hamid, R., & Fuentes, H. R. (1996). Use of Geographic Information Systems (GIS) in water resources: A review. *Water Resources Management*, *10*(4), 251–277. doi:10.1007/BF00508896

United States Geological Survey. (2006). Mount St. Helens after 5/18/80 eruption. Retrieved from http://ned.usgs.gov/Ned/historic.asp

United States Geological Survey. (2014). The Water Cycle. Retrieved from http://water.usgs.gov/edu/watercycle.html

US Environmental Protection Agency. (2009). *Technical Guidance on Implementing the Stormwater Runoff Requirements for Federal Projects under Section 438 of the Energy Independence and Security Act*.

Yin, J., Yu, D., Yin, Z., Wang, J., & Xu, S. (2012). Multiple scenario analyses of Huangpu River flooding using a 1D/2D coupled flood inundation model. *Natural Hazards*, *66*(2), 577–589. doi:10.1007/s11069-012-0501-1

Vita

Carlos Galdeano Alexandres grew up in Mexico City, where he attended the Modern American School. He earned his Bachelor of Science degree in Civil Engineering from the National Autonomous University of Mexico, and worked in the environmental and financial consulting industries before returning to school. Carlos is now completing his Master of Science degree in Environmental and Water Resources Engineering at The University of Texas at Austin, where he will continue to pursue his doctoral degree in Civil, Architectural, and Environmental Engineering. Carlos master's work has been founded by the National Council of Science and Technology (CONACyT) in Mexico.

Permanent email: cgaldeano@utexas.edu

This thesis was typed by the author